GRAPHENE OXIGE BASED MEMBRANE FOR WATER PURIFICATION

BY

OMER ALNOOR OSMAN ALAMEEN

A Thesis Presented to the
DEANSHIP OF GRADUATE STUDIES

KING FAHD UNIVERSITY OF PETROLEUM & MINERALS

DHAHRAN, SAUDI ARABIA

In Partial Fulfillment of the
Requirements for the Degree of

MASTER OF SCIENCE

In

MECHANICAL ENGINEERING

May, 2017

KING FAHD UNIVERSITY OF PETROLEUM & MINERALS

DHAHRAN- 31261, SAUDI ARABIA

DEANSHIP OF GRADUATE STUDIES

This thesis, written by **Omer Alnoor Osman Alameen** under the direction of his thesis advisor and approved by his thesis committee, has been presented and accepted by the Dean of Graduate Studies, in partial fulfillment of the requirements for the degree of **MASTER OF SCIENCE IN MECHANICAL ENGINEERING.**

Dr. Zuhair Mattoug Gasem
Department Chairman

Dr. Khan, Zafarullah
(Advisor)

4/6/17

Dr. Salam A. Zummo
Dean of Graduate Studies

Dr. Laoui, Tahar
(Member)

Dr. Khaled, Mazen
(Member)

20/4/2017
Date

© Omer Alnoor Osman

2017

I dedicate this thesis to my family

ACKNOWLEDGMENTS

First of all, I want to express my genuine appreciation to my advisor Professor. Zafarullah Khan my Co-Advisor Professor Tahar Laoui for the endless support of my M.Sc. study, for his understanding, inspiration and massive knowledge. Also, I would love to thank the committee member Professor. Mazen Khalid, for the continuous support and insightful comments.

Moreover, I wish to acknowledge Dr. Ahmed Ibrahim, Dr. Feras Kafiah and Dr. Hafizzahid Shafi for the exceptional comments and the great help I received to complete my research studies.

At long last, I should express my appreciation to my family for their endless support during this study period. This achievement would not have been conceivable without them.

Omer Alnoor Osman

TABLE OF CONTENTS

ACKNOWLEDGMENTS ..... **V**

TABLE OF CONTENTS ..... **VI**

LIST OF TABLES ..... **VIII**

LIST OF FIGURES ..... **IX**

LIST OF ABBREVIATIONS ..... **XI**

ABSTRACT ..... **XIII**

ملخص الرسالة ..... **XV**

CHAPTER 1 INTRODUCTION **1**

1.1 Membrane Separation Technology **1**

1.2 Graphene Oxide-based material **3**

1.3 Graphene oxide based membrane for water filtration **6**

1.4 Objectives **7**

1.5 Thesis outline **8**

CHAPTER 2 LITERATURE REVIEW **9**

2.1 Freestanding GO-based membrane **9**

2.2 GO for membrane surface modification **12**

2.3 GO-incorporated composite membrane **16**

2.4 Adhesion improvement of GO with polymeric substrates **19**

2.5 Plasma treatment **20**

CHAPTER 3 EXPERIMENTAL WORK **24**

3.1 Materials **24**

3.2 Substrate preparation **24**

3.3 GO and rGO coated PES membrane preparation **25**

3.4 GO/PAM and rGO/PAM coated PES **26**

3.5 Characterization of membrane properties **27**

3.6 Membrane performance evaluation **28**

3.7 Static bacteria adhesion test **30**

CHAPTER 4 RESULTS AND DISCUSSION **32**

4.1 Modification of membrane support **32**

4.2 Characterization of the GO-PES membranes **34**

4.3 Diffusion study results for the GO/PES membrane **37**

4.4 Diffusion study results for the rGO/PAM coated PES membrane **47**

4.5 Static bacteria adhesion test results **52**

CHAPTER 5 CONCLUSIONS AND RECOMMENDATIONS **54**

5.1 Conclusions **54**

5.2 Recommendations **55**

REFERENCES **57**

VITAE **66**

LIST OF TABLES

Table 2.1 Chemicals used to stabilize GO on membranes surfaces. 20
Table 4.1 The diffusion rate of KCl salt ions through prepared membranes..... 40
Table 4.2 The diffusion rate of KCL ions through prepared 1, 3 and 5 D.C rGO/PES membranes..... 46

LIST OF FIGURES

Figure 1.1 Graphene oxide chemical structure[22].....4
Figure 1.2 Water transport through GO nano channels [36]. 5
Figure 2.1 (a) Graphene oxide (GO) sheet. (b) The polyallylamine structure of. (c) A colloidal suspension of (left) GO and (right) PAA+GO. (d) PAA-modified GO paper cross section view [57]. 11
Figure 2.2 (a) Illustration of the drug-loaded film formation via a vacuum filtration process. (b) Bent prepared a film. (c) images of the GO film, the graphene oxide–polyethyleneimine hybrid (GPH) film and the Ciprofloxacin (CF)- loaded GPH film [50]. 11
Figure 2.3 Schematic illustration of layer-by- layer assemblies of (GO) coating on a polyamide active layer membrane [19].....13
Figure 2.4 Schematic illustrating of (a) chemical cross-linking (b) Graphene oxide deposition on PEI via dip-coating technique to form the selective layer[57].....14
Figure 2.5 Schematic illustration GO / PAH formed on booth surfaces of hydrolyzes polyacrylonitrile hPAN support via layer by layer deposition technique[60]. 15
Figure 2.6 Schematic illustration of amide bond formation chemical reaction between Cs chain and GO [28] 15
Figure 2.7 SEM images of PVP /PVDF/GO top surface membranes at different GO amount added. (a-1, a-2) 0.2 wt%, (b-1, b-2) 0.5 wt%, (c-1, c-2) 1.0 wt% and (d-1, d-2) 2.0 wt%. [37]. 18
Figure 2.8 SEM images for PES surfaces: (a) before treatment, (b) after 5 min plasma treatment , (c) after 15 min plasma-treatment, (d) after 30 min plasma-treatment [42] 23
Figure 3.1 Schematic diagram showing spin coating steps of GO layers on substrate surface 26
Figure 3.2 GO reduction process via exposure to HI vapor. 26
Figure 3.3 Diffusion cell 2D view 30
Figure 4.1 SEM and AFM micrographs of (a, e) bare PES, (b, f) 2min PT PES, (c, g) 10min PT PES, (d, f) 20min PT PES.....34
Figure 4.2 SEM cross-sectional view of PES as function of PT time (a) bare PES, (b) 2 min-PT, (c) 10 min, (d) 20 min.....34
Figure 4.3 FESEM images at low and high magnification for representative parts of fully covered PES substrate surface (a, e), (b, f), (c, g) and (d, h) for O on Bare PES surface and PES PT 2, 10 and 20 min respectively.....36
Figure 4.4 High magnification SEM images for GO coated PES and glass slice at different PH values. 37

Figure 4.5 Cross-sectional SEM image of GO/PES membrane. (a, b) for one coating deposition cycle, (c, d) three coating deposition cycles at different magnifications. 37
Figure 4.6 The diffusion study results for bare and plasma treated PES for 2, 10 and 20 min. 38
Figure 4.7 The diffusion study results of KCl ions through GO/PES-PT samples. 39
Figure 4.8 Blockage percentage of KCl ions through PT PES and GO PES samples. 40
Figure 4.9 SEM images of GO/PES sample on Bare PES surface and PES PT 2 min, 10 min and 20 min respectively. GO detached flakes are indicated by arrows in panels (a, c), where the diameter of active membrane area is about 3 mm. It is clear that 2 and 20 min PT yielded 42
Figure 4.10 FTIR spectra for Bare PES and GO/PES membranes samples respectively. 43
Figure 4.11 Digital photos for PES, GO/PES, and rGO/PES membranes. 43
Figure 4.12 FESEM of rGO coated 2min PT PES membrane surface (a, b) and (c, d) at different magnifications before and after the diffusion test, (e) is the diffusion study result for the sample before the diffusion and (f) is FTIR result for the same sample. 45
Figure 4.13 (a) Diffusion study results for 1, 3 and 5 deposition cycles (D.C) of rGO on PES 2 min PT (b) DI-water permeation through the membranes at 10 bar. 46
Figure 4.14 SEM images showing the cross-section view of the rGO/PAM coated PES for (a) 2H sample and (b) 2L sample. 47
Figure 4.15 Diffusion study results of the KCl ions passing through the prepared 2L rGO/PAM-PES samples (a) at 25 ℃ HI solution and (b) at 80 ℃ HI solution. 48
Figure 4.16 Diffusion study results of the KCl ions passing through 2H rGO/PAM-PES samples (a) at 25 ℃ HI solution and (b) at 80 ℃ HI solution. 49
Figure 4.17 KCl ions rejection percentage results as a comparison between 2L and 2H samples reduced by HI vapor while HI solution was maintained (a) at 25 ℃ and (b) at 80℃. 50
Figure 4.18 The permeated water flux through the 2H samples reduced at 80 ℃ for different time intervals. 51
Figure 4.19 SEM image of a representative surface area after 3 hours of immersion in the bacteria solution for (a) Bare PES, (b) GO/PAM-PES, (c) 2H reduced for 0.25-hr, (d) 2H reduced for 0.5-hr, (e) 2H reduced for 1-hr and (f) 2H reduced for 2-hr. 53

LIST OF ABBREVIATIONS

GO: Graphene oxide.

rGO: reduced Graphene oxide.

PES: Polyethersulfone

LBL: Layer by layer

FO: forward osmosis

RO: reverse osmosis

VUV: vacuum ultraviolet

DC: deposition cycle

PT: Plasma treatment

PAM: Polyacrylamide

ABSTRACT

Full Name : Omer Alnoor Osman Alameen

Thesis Title : Graphene Oxide based membrane for water purification

Major Field : Materials and manufacturing

Date of Degree : January 2017

Here we report the synthesis of graphene oxide (GO)/polyether sulfone (PES) membrane showing enhanced GO to PES adhesion aimed at water purification application. A simple air plasma treatment enabled us to modify the surface characteristics (surface cleanliness, wettability, and porosity) of the PES substrate and improve the adhesion of GO layers on PES. GO/PES membrane was prepared via layer-by-layer (LBL) deposition of GO on plasma treated PES using spin coating technique. The effect of plasma treatment (PT) with different times (2, 10 and 20 min) on the surface cleanliness, wettability and pore structure of treated PES substrate was investigated via atomic force microscopy (AFM), scanning electron microscopy (SEM), Fourier Transform infrared spectroscopy (FTIR), and contact angle goniometry (CA). The membrane performance was evaluated by measuring the potassium chloride (KCl) ions transport through the GO/PES membrane. A 2-min plasma treatment of PES substrate showed the best adhesion and stability of deposited GO layers and ~57% KCl ions blockage with three layer-by-layer deposition cycles. This low ions blockage was attributed to the extensive cracks found in the deposited GO layers. The use of reduced graphene oxide (rGO) instead of GO helped in producing defect-free rGO/PES membranes with ~94% KCl ions blockage for three deposition cycles. This ions blockage improved to ~99% with five layer-by-layer deposition cycles. The use of positively charged polyacrylamide (PAM) as

an adhesive layer by spin coating PAM on PES membrane surface had further improved GO and rGO stability on PES membrane surface. The anti-bacterial properties and reduction time effect on the selectivity of the prepared GO/PAM and rGO/PAM coated PES were also investigated. The results proved that all GO/PAM and rGO/PAM coated PES membranes exhibited good antibacterial properties. Moreover, it was clearly observed that, as GO reduction time and GO layers' thickness increased, KCl ions blockage increased and the permeated water flux decreased.

ملخص الرسالة

الاسم الكامل: عمر النور عثمان الأمين

عنوان الرسالة: غشاء أكسيد الجرافين لتنقية المياه

التخصص: علم المواد والتصنيع

تاريخ الدرجة العلمية: يناير 2017

في هذا البحث نعرض عملية تصنيع اغشية أوكسيد الجرافين\متعدد ايثر السلفون الذي يظهر تعزيز التصاق اكسيد الجرافين مع متعدد ايثر السلفون والمعد للاستخدام في تطبيقات تنقية المياه. المعالجة البسيطة باستخدام البلازما مكنتنا من تعديل خصائص السطح (نظافة السطح ، الترطيب والمسامية) لعينات متعدد ايثر السلفون كما مكنتنا من تحسين التصاق طبقات أكسيد الجرافين مع متعدد ايثر السلفون.

تم إعداد غشاء أكسيد الجرافين\متعدد ايثر السلفون عن طريق استخدمنا اسلوب الطبقة بقرب الطبقة بواسطة تقنية النسج بالدوران. تمت دراسة تاثير المعالجة بالبلازما على نظافة السطح الترطيب والتكوين المسامي للعينات التي تمت معالجتها عند فترات زمنية مختلفة للمعالجة (دقيقتين, عشر دقائق وعشرون دقيقة) باستخدام مجهر القوة الذرية (AFM),المجهر الإلكتروني الماسح (SEM) و جهاز "فوريير" لتحويل طيف الأشعة تحت الحمراء (FTIR) وجهاز قياس زاوية التلامس.

تم تقييم الأداء من خلال قياسل معدل انتقال أيونات كلوريد البوتاسيوم خلال أغشية أكسيد الجرافين\متعدد ايثر السلفون. أظهرت علاج سطح متعدد إيثر السلفون بالبلازما لمدة دقيقتين أفضل نتائج التصاق والاستقرار لطبقات أكسيد الجرافين (ثلاث دورات ترسب طبقة تلو طبقة) و ما يقارب ال 57٪ تعطيل لأيونات كلوريد البوتاسيوم. ويعزى معدل التعطيل المنخفض هذا إلى الشقوق الكثيرة الموجودة في طبقات أكسيد الجرافين. ساعد استخدام أكسيد الجرافين المختزل بدلا من أكسيد الجرافين في إنتاج أغشية أكسيد الجرافين المختزل\متعدد ايثر السلفون, الخالية من العلل مع ما يقارب ال 94٪ تعطيل لأيونات كلوريد البوتاسيوم (ثلاث دورات ترسب طبقة تلو طبقة). هذا التعطيل لأيونات كلويد البوتاسيوم تحسنت إلى ما يقارب ال 99٪ في العينات التي تم تحضيرها بواسطة خمس دورات ترسب طبقة تلو طبقة.

استخدام البولي أكريلاميد موجبة الشحنة (PAM) باعتبارها طبقة لاصقة عن طريق اسلوب النسج بالدوران لمحلول البولي أكريلاميد على غشاء متعدد ايثر السلفون عمل على تحسين استقرار أكسيد الجرافين وأكسيد الجرافين المختزل على سطح غشاء متعدد ايثر السلفون. تم أيضا دراسة الخصائص المضادة للبكتيريا وتأثير مدة الاختزال على الانتقائية غشاء متعدد إيثر السلفون والمغلف بأكسيد الجرافين\ البولي أكريلاميد و أكسيد الجرافين المختزل\ البولي أكريلاميد . أثبتت النتائج أن جميع العينات اظهرت خصائص مضادة للبكتيريا جيدة. وعلاوة على ذلك، لوحظ بشكل واضح أنه مع زيادة سمك طبقات أكسيد الجرافين و مدة اختزال اوكسيد الجرافين ، يزيد معدل إعاقة أيونات كلويد البوتاسيوم ويقل معدل نفاذ المياه.

CHAPTER 1

INTRODUCTION

By 2050, the human population is estimated to reach 10 billion since the population is increasing rapidly. Consequently, the demand for sweet water will increase leading to the potential water crisis. About (97%) of the earth's water resources are sea water which means that sea water desalination is the most likely method for obtaining fresh water supplies [1].

1.1 Membrane Separation Technology

A membrane is a selective barrier to some elements while allowing others to pass through. The membrane performance can be described by its selectivity and permeated flux. However, both of these parameters should be simultaneously considered for membrane usage economics. Water flux can be defined as the permeation rate of the water that passes through a membrane. High membrane productivity requires a high permeation flux while the selectivity of a membrane is related to the ability of the membrane to eliminate certain components from a solution mixture.

Generally, membranes can either be classified according to their degree of asymmetry and porosity or according to their origin (organic or inorganic membrane). A breakthrough has been made in membrane separation technology by the invention of a polymeric asymmetric flat sheet membrane which can be fabricated at low cost and high

packing density. This breakthrough was very beneficial for a large scale application [2]. Nevertheless, some weak points such as high-pressure compressibility, low stability under severe chemical environments and elevated temperatures have placed a limitation on their widespread usage in various industrial applications.

Membranes used for water desalination can be classified into membrane distillation, electrodialysis, microfiltration, ultrafiltration, nano-filtration and reverse osmosis [3]. Reverse osmosis (RO) is the most effective water filtration process with equitable energy consumption and high salt rejection percentage. Nowadays energy consumption for this technique is about 1.8 kW h/ m^3 , which is relatively high [4]. RO technique has the drawback of membrane fouling which significantly affects membrane performance.

Graphene oxide (GO) is believed to be a good candidate for use as a membrane's material for a water filtration application since it is only one carbon atom thick (around 1.1 ± 0.2 nm) which reduces permeation resistance and increases the flux [5]. GO layers are also known to have good mechanical properties[6], chemical and thermal stability [7][8] with unique antifouling and antibacterial properties due to its hydrophilic nature which made it applicable and very useful candidate to overcome RO fouling problem [9]. Thus, it can be designed to be permeable to either water or water vapor and to reject other unwanted molecular species [10]. Different techniques have been used to deposit GO layers on the membrane's surfaces as an active selective layer for filtration applications. Spin coating technique is one of the most applicable effective methods to produce a uniformly distributed thin film coating layer on a planner substrates surface[11]. This technique has widely opened the ability to produce thin film composites (TFC) membranes for a variety of different applications. This technique is comparable to

other techniques used to provide TFC membranes, such as layer by layer (LBL) dip coating, which have been used for pervaporation water filtration[12][13], reverse osmosis (RO)[14][15], nanofiltration [16] and gas separation applications[17][18]. Spin coating deposition technique is simple, environmentally friendly and less time consuming when compared to LBL dip coating which has the drawback of poor film thickness control. TFC membranes fabricated for water filtration application via LBL deposition technique suggested that the mechanism of ions rejection by outermost layer is due to the Donnan exclusion principle [19]. However, recently the experimental results proved that ions or water rejection and permeation for some LBL membranes should better be described by solution diffusion principle [20].

In this work, spin coating technique is used to deposit GO layer on PES membrane after conducting plasma treatment to improve GO layer stability on PES surface. Moreover, polyacrylamide (PAM) is used to crosslink GO layer with PES surface for further adhesion improvement to withstand the water high pressure applied during RO water filtration application without GO degradation.

1.2 Graphene Oxide-based material

Graphene oxide (GO) is two dimensional element composed of oxygen, hydrogen and carbon at different proportions (between 2.2 - 2.9 C:O ratio) [21]. It is a single layer of graphite oxide with a thickness of around 1.1 ± 0.2 nm. The defects and edges of every layer are ended by hydroxyl, carbonyl and carboxyl groups as shown in **Figure** 1.1[22].

Different methods were used to prepared GO such as the Brodie method [23], the Staudenmaier method [24], and the Hummers or modified Hummers methods [21][25][26][27]. The common technique used to prepare GO by this method was graphite oxidation with a strong oxidant in an acidic medium. Each method used produced GO at a different C:O ratio[28]. Within the graphite structure, the interlayer spacing is about 0.34 nm between two neighbored graphene sheets [29]. The interlayer spacing value between GO layers was found to be higher than graphite, this could be related to the introduced oxygen functional groups after the oxidation process. The

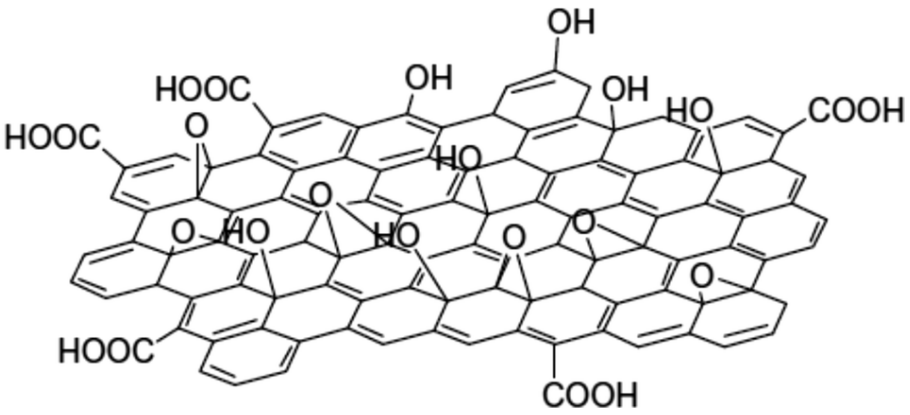

Figure 1.1. Graphene oxide chemical structure[22].

interaction between water molecules and hydroxyl GO functional groups in relatively high humidity environments can increase interlayer spacing from 0.6 to 1.2 nm [30]. The ultrasonication process can be used to homogeneously exfoliate graphite oxide in water and produce an aqueous solution [31]. Graphite oxide can also be exfoliated in organic solvents as well as some polar solvents, such as dimethylformamide, ethylene glycol, and N-Methyl pyrrolidone [32][33].

The graphene-like structure, reduced graphene oxide (rGO), can be produced by thermal reduction of GO [34][35]. Certain chemicals can also be used for chemical GO reduction such as a hydriodic acid (HI) [36], NABH4 [37], hydrazine [38], and hydroquinone [39]. Unlike pristine graphene, rGO contains a significant number of residual oxygen functional groups as evidenced by elemental analysis results.

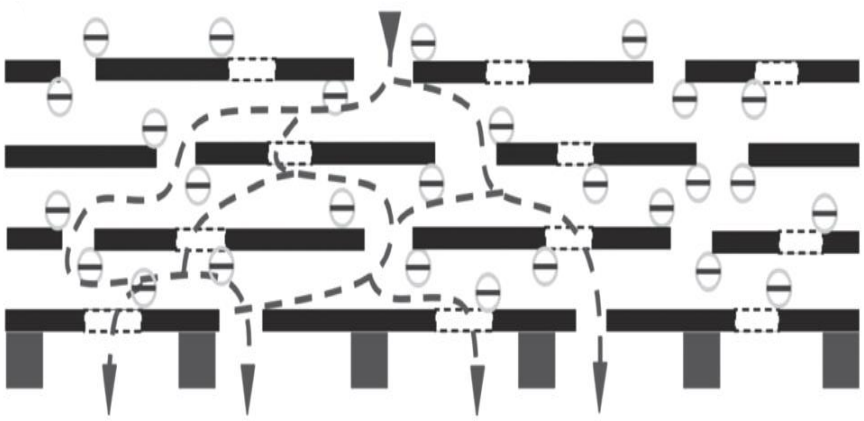

Figure 1.2. Water transport through GO nano channels [36].

GO layers are known to be chemically stable in water which has made their utilization in membrane applications possible [7]. In addition, GO layers allow the water to permeate through its 2D nanochannels as shown in **Figure** 1.2**.** This property introduces significant enhancement in the water desalination application and gives more opportunities to overcome the RO water desalination challenges[40][41]. The graphene oxide based membrane in liquid separation application was proven to be a success and is very promising due to its unique size sieving effect.

1.3 Graphene oxide based membrane for water filtration

Graphene oxide based membranes have been used in different applications such as gas separation [42][43][44], water desalination [45][46][47] and heavy metal removal [48][49][50]. Regarding water filtration, **Nicolaï et al.** [51] reported that free standing GO membranes are excellent candidates for RO water desalination applications, relying on their molecular dynamics simulations (MDS) results. The salt rejection for this type of membrane reached up to 100% with double water permeation compared to other commercial RO membranes. **Kim et al.** [52] modified the surface of amino polyethersulfone (aPES) by GO layer followed by another amino GO (aGO) layer by using the layer-by-layer (LbL) self-assembly technique. The obtained modified RO membrane showed a significant enhancement of chlorine resistance when compared to the commercial polyamide (PA) RO membrane, and about a 98% salt rejection with 28 $L/m^2.h$ water flux. **Zhao et al.** [53] verified that the incorporation of GO nanosheets into a DMAc/PVDF polymer solution had enhanced the fabricated membrane surface. The Bovine serum albumin (BSA) rejection for the resultant composite membranes was 44.3% and the water flux was 26.49 L/ m2 h. The antifouling properties were noticeably enhanced when compared to the pristine PVDF membrane.

Han et al.[54] converted GO into reduced GO (rGO) by mixing a GO solution with NaOH. The mixture was stirred and heated in the presence of a nitrogen gas flow until rGO dispersion was obtained. A free-standing ultrathin rGO membrane with 22 to 53 nm thickness was then fabricated via the vacuum filtration deposition

technique. A dead-end filtration cell was used to evaluate the developed rGO membrane performance. The permeated water flux was 21.8 L/ (m^2 h. Bar) with (>99%) organic dyes rejection and (20 to 60%) NaCl salt rejection.

Joshi et al.[55], [56] developed GO membranes which were able to block solutes larger than 0.45 nm hydrated radii under wet condition. Diffusion rates of smaller ions through the fabricated membrane were found to be 1000 times faster than simple diffusion rate expectations. This behavior was related to the hydrated enlarged 2D capillaries which acted as a mechanical sieve allowing only ions of the correct size.

1.4 Objectives

- Development of a nano-filtration graphene oxide (GO) based membrane with improved GO adhesion and stability on the polyether sulfone (PES) polymeric porous substrate for water purification application.
- Optimization for the parameters that affect the adhesion and stability of GO layers on the PES substrate surface.
- Investigation of the plasma treatment effect on both the membrane surface morphology and adhesion enhancement of deposited GO layers to the underlying PES substrate surface.
- Improvement for both GO and rGO stability on PES membrane surface by using positively charged polyelectrolytes to withstand the high water pressure in revers osmosis (RO) water filtration application.

- Evaluation of the antibacterial properties and the performance of the fabricated GO-based membrane regarding salt ions rejection.

1.5 Thesis outline

- Chapter 1 present an introduction about the importance of securing fresh water, membrane separation technology and GO based membranes for water filtration.
- Chapter 2 contains a literature review of previously reported GO-based membranes along with different methods used to immobilize GO on various substrates surface.
- Chapter 3 contains a description of the experimental work performed to prepare the PES substrate, fabricate the GO/PES and rGO/PES membranes and evaluate their performance.
- Chapter 4 includes the results and the discussion sections.
- Chapter 5 includes the conclusion and recommendations.

CHAPTER 2

LITERATURE REVIEW

Graphene oxide based membranes have been utilized in water purification applications in different ways. They have been fabricated as a free standing membrane paper like material, deposited on a membrane substrate surface using different techniques and incorporated within the membrane matrix to fabricate composite membranes.

2.1 Freestanding GO-based membrane

In this type of GO-based membrane, GO is used directly as an effective selective layer. One of the most common techniques used to prepare free-standing GO-based membranes is vacuum filtration. **Park et al.** [57] prepared a free standing GO-based membrane showing an excellent mechanical stiffness and strength via simple filtration where graphene oxide was chemically cross-linked with polyallylamine as shown in **Figure** 2.1. **Hu et al.** [58] found that large-scale production of a GO paper like material could be achieved by a simple drop casting technique on hydrophobic surfaces. A small amount of glutaraldehyde (<10 wt %) had enhanced the mechanical stiffness by 341% and fracture strength by 234% when compared to unmodified GO paper. **Nair et al.** [59] indicated that a free standing GO-Copper membrane was fabricated by spray coating GO laminates on a copper (Cu) foil then chemically etching the copper to obtain a GO sheet. The resultant fabricated membranes showed a high water permeability while blocking liquids, vapors, and gas permeation.

Sun et al. [49] used the drop-casting technique to prepare a GO nanofiltration (NF) membrane with an interlayer spacing of ~0.82 nm. These membranes were efficiently used for sodium salt separation from organic contaminants. Recently, **Nicolaï et al.** [51] reported that free standing GO membranes are excellent candidates for RO water desalination membranes, relying on their molecular dynamics simulations (MDS) results. The salt rejection for this type of NF membranes reached up to 100% with doubled water permeation compared to other RO membranes. **Sungjin Lee et al.** [60] also found that the mechanical stiffness could be enhanced from 10% to 200% and the fracture strength by 50% with a less than 1 Wt.% Mg^{2+} and Ca^{2+} modification of graphene oxide paper.

Huang et al. [61] have developed a free standing GO membrane cross-linked by PEI (polyethyleneimine) to be used for a drug delivery system prepared via a one-step preparation technique as shown in **Figure** 2.2**. Xu et al.** [62] have developed a composite membrane composed of GO and TiO_2 nanoparticles with an average pore size of about 3.5 nm. This membrane showed a high rejection performance (100%) for both methyl orange and Rhodamine.

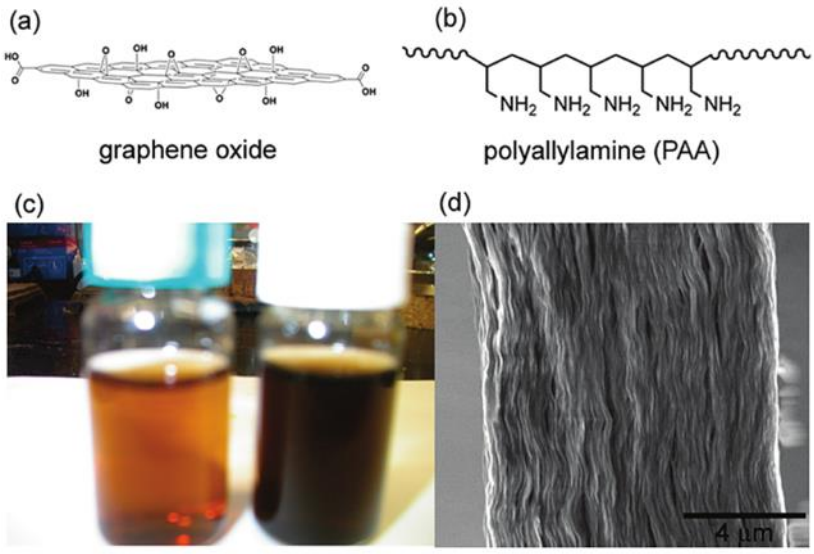

Figure 2.1. (a) Graphene oxide sheet. (b) The polyallylamine structure of. (c) A colloidal suspension of (left) GO and (right) PAA+GO. (d) PAA-modified GO paper cross section view [57].

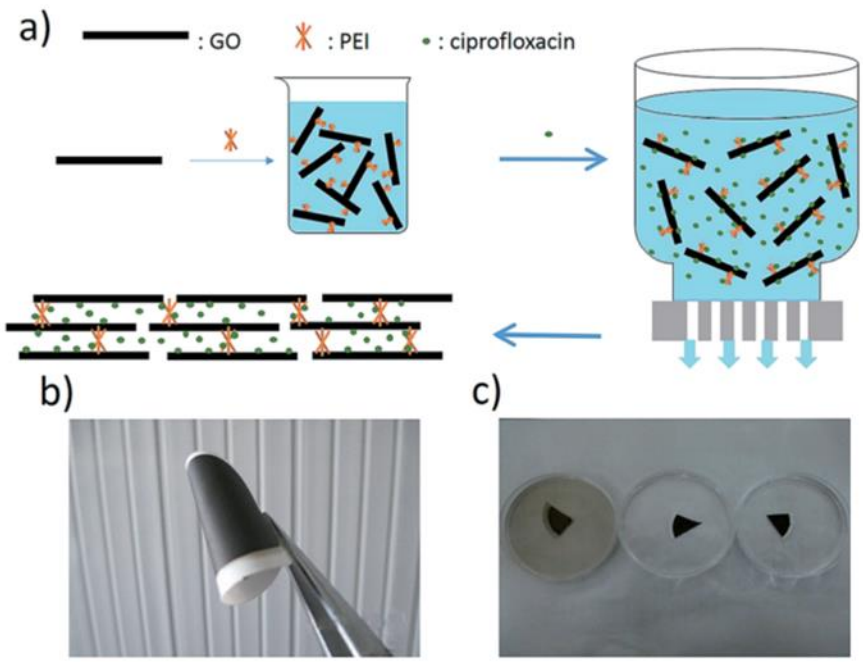

Figure 2.2. (a) Illustration of the drug-loaded film formation via a vacuum filtration process. (b) Bent prepared a film. (c) images of the GO film, the graphene oxide–polyethyleneimine hybrid (GPH) film and the Ciprofloxacin (CF)- loaded GPH film [50].

2.2 GO for membrane surface modification

For this type of GO-based membrane, GO layers were deposited on a membrane substrate surface to improve membrane performance in terms of hydrophilicity, antibacterial, antifouling and chlorine resistance [63]. **Choi et al.** [14] utilized the same technique to modify the PA-thin film composite (TFC) membrane as shown in **Figure** 2.3**.** The GO layers improved both antifouling and membrane chlorine resistance, with the same separation performance. GO and TiO_2 nanoparticles were used by **Gao et al.** [64] to modify the polysulfone membrane surface via the LbL-SA method.

The antibacterial properties of the GO modified membrane surface were further studied by **Perreault et al.** [65]. GO nano-flakes were covalently bonded to a PA thin layer to achieve a 65% inactivation of the bacterial cells after one hour, without affecting the membrane salt rejection or the water flux. **Hung et al.** [40] studied the improvement of GO-surface medication on pervaporation membranes. A pressure-assisted self-assembly technique was used to obtain multilayers of GO on the hydrolyzed polyacrylonitrile (PAN) surface. The obtained membrane showed 99.5 wt% water recovery and the water flux was 4137 g/m^2.h. **Chunlin Zhao et al**. [66] used a simple drop-casting technique to form uniform layers of reduced graphene oxide (RGO) on the top of polydopamine-coated polyethylene terephthalate (PET) substrates.

Goh et al. [67] deposited GO on a poly(amide-imide)–poly ethylenimine (PAI–PEI) hollow fiber membrane as shown in **Figure** 2.4. The results revealed that the GO layers worked as effective selective barriers with a relatively high water permeability of up to 86%. The GO deposited film showed good stability when it was exposed to a

backwashing pressure of around 1 bar with a 600 mL/min cross-flow rate. **Xia et al.** [68] incorporated GO into the polyamide (PA) active layer of a PSF membrane via interfacial polymerization reaction. The resultant membrane showed a high water flux, anti-fouling performance, and a high natural organic matter NOM removal rate.

Hu and Mi [69] have modified the surface of a polydopamine-coated polysulfone membrane by a technique using GO cross-linked with 1,3,5-benzenetricarbonyl tri-chloride via layer-by-layer. The membrane water flux was about 4-10 times higher than most of the commercial NF membranes (between 80 and 276 LMH/MPa). The monovalent and divalent salts rejection levels were relatively low (6−46%) but the Rhodamine-WT rejection level was high (93−95%).

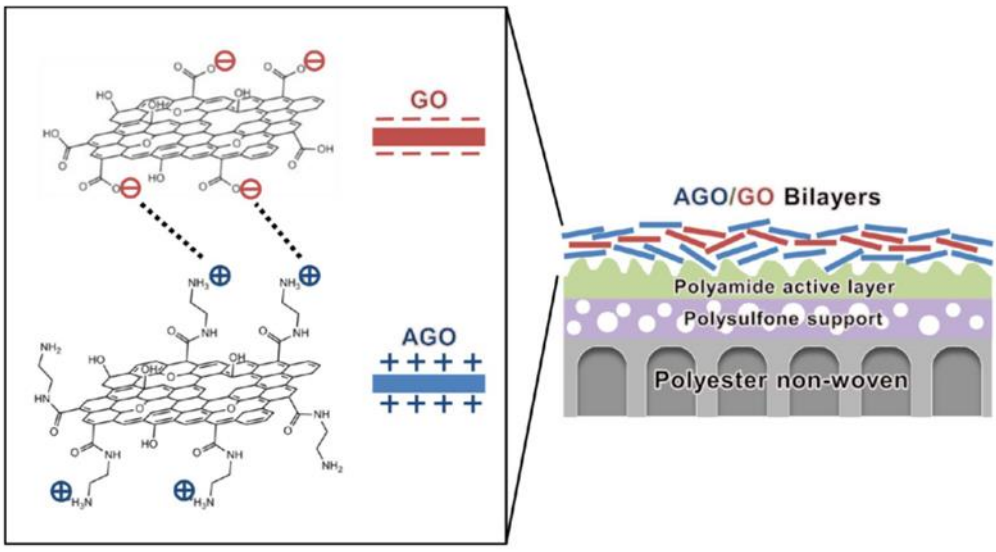

Figure 2.3.Schematic illustration of layer-by- layer assemblies of (GO) coating on a polyamide active layer membrane [19]

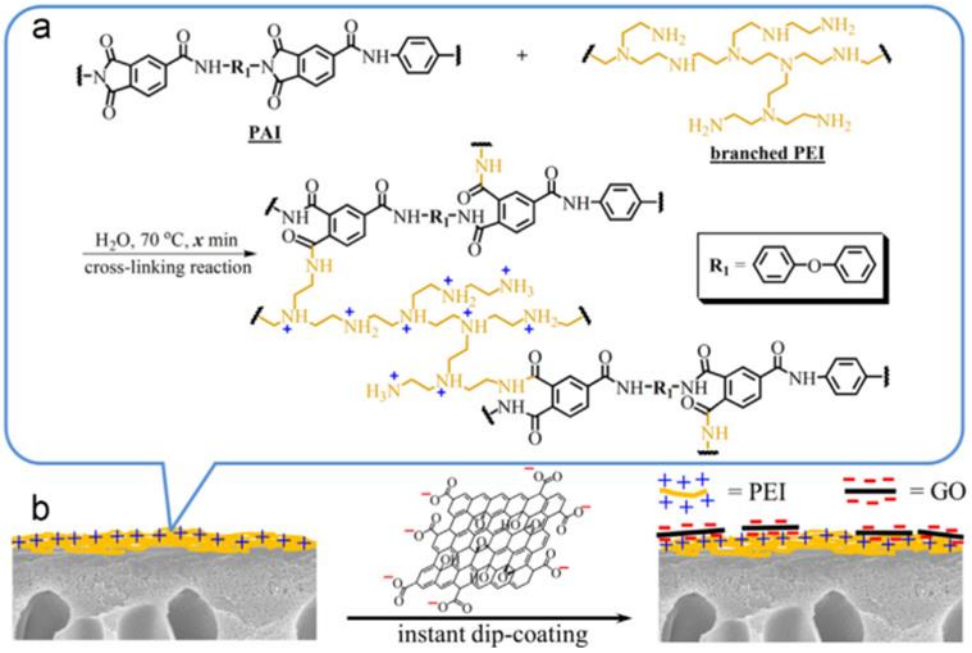

Figure 2.4.Schematic illustrating of (a) chemical cross-linking (b) Graphene oxide deposition on PEI via dip-coating technique to form the selective layer[57].

Hu and Mi [70] fabricated, via a layer-by-layer assembling method, a GO/ poly (allylamine hydrochloride) (PAH) coated poly(acrylonitrile) membrane as shown in **Figure** 2.5**.** An electrostatic interaction took place between the negatively charged GO and the positively charged (PAH). FO was used to investigate the resultant membrane performance. The water permeability was found to be double that of commercial FO membranes. **Bhadra et al.** [71] studied GO immobilization on the surface of the polytetrafluoroethylene (PTFE) membrane. The performance of the resultant membrane was investigated in a direct contact membrane distillation application. The modified membrane revealed significant enhancement of the water permeate flux (97 kg/m^2.h at 80 °C) with 100% salt rejection. **Hegab et al.** [72] also studied the antifouling properties of a PSF membrane modified by GO functionalized chitosan as shown in **Figure** 2.6. The

resultant membrane exhibited higher performance when compared to the unmodified membrane in terms of water flux, salt rejection (NaCl) and antifouling properties.

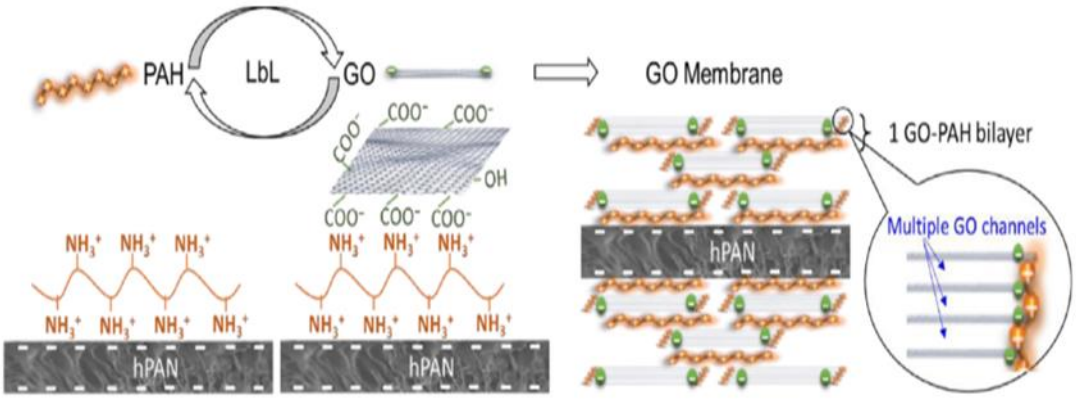

Figure 2.5.Schematic illustration GO / PAH formed on booth surfaces of hydrolyzes polyacrylonitrile hPAN support via layer by layer deposition technique[60].

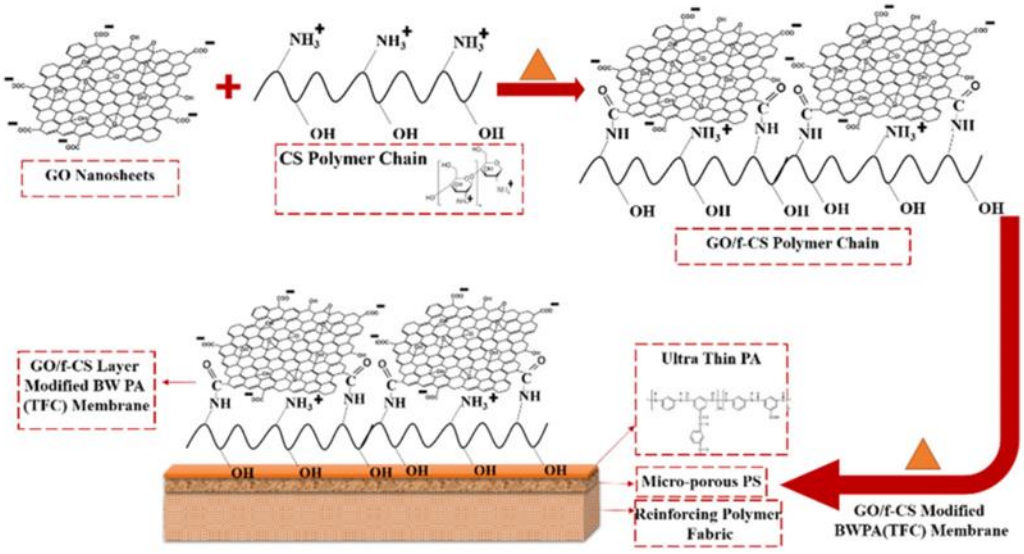

Figure 2.6.Schematic illustration of amide bond formation chemical reaction between Cs chain and GO [28]

2.3 GO-incorporated composite membrane

In this type of GO base membrane, the GO layers are incorporated with the membrane bulk material. The water permeability, mechanical and antimicrobial membrane properties were improved by the presence of GO inside the polymer matrix [73][74]. The functionalization of GO could be done either before polymer matrix inclusion or mixed directly with the matrix. **Yu et al**. [41] used hyperbranched polyethyleneimine for GO functionalization. In another study conducted by **Xu et al.** [75], 3-amino propyl tri ethoxy silane and isocyanate were used. **Zhao et al.** [76] studied the effect of various ratios of GO incorporated in polyvinylidene fluoride (PVDF) and polysulfone (PSF) mixer solutions before casting. The resultant fabricated membranes were tested the via phase inversion method. The GO/PVDF rejection performance for serum albumin (BSA) was 57% and 95% for GO/PES.

The antifouling properties were enhanced by GO addition due to the improvement in wettability and surface roughness of the membranes. Non-functionalized GO was incorporated into N-methyl pyrrolidone (NMP)/PSF prepared by the wet phase inversion method [77]. The resultant membrane surface was moderately hydrophilic and the salt rejection had improved (72% rejection of Na2SO4 at the applied pressure of 4 bars). Another study of GO incorporation into the polymer matrix was carried out by **Zinedine et al.** [78]. They fabricated GO /dimethylacetamide /polyether sulfone (PES) composite membrane NF membranes via the phase inversion method. This membrane at 0.5 wt% of GO addition showed a high water flux, fouling resistance and dye removal capacity when compared to unmodified PES. **Jun et al.** [79] fabricated GO/ PSF forward osmosis (FO) membranes followed by the formation of a Polyamide (PA) active layer on the composite

membrane by interfacial polymerization. The water permeability was improved due to the hydrophilicity improvement of the membrane.

Liu et al. [80] in their research had introduced GO/polyvinyl pyrrolidone into (PVDF) membranes which were fabricated via the immersion precipitation technique. The porosity and hydrophilicity of the membrane surface can be controlled by the amount of GO wt% additions as shown in **Figure** 2.7**.** Moreover, the resultant membrane exhibited high absorbability for Methylene blue particles.

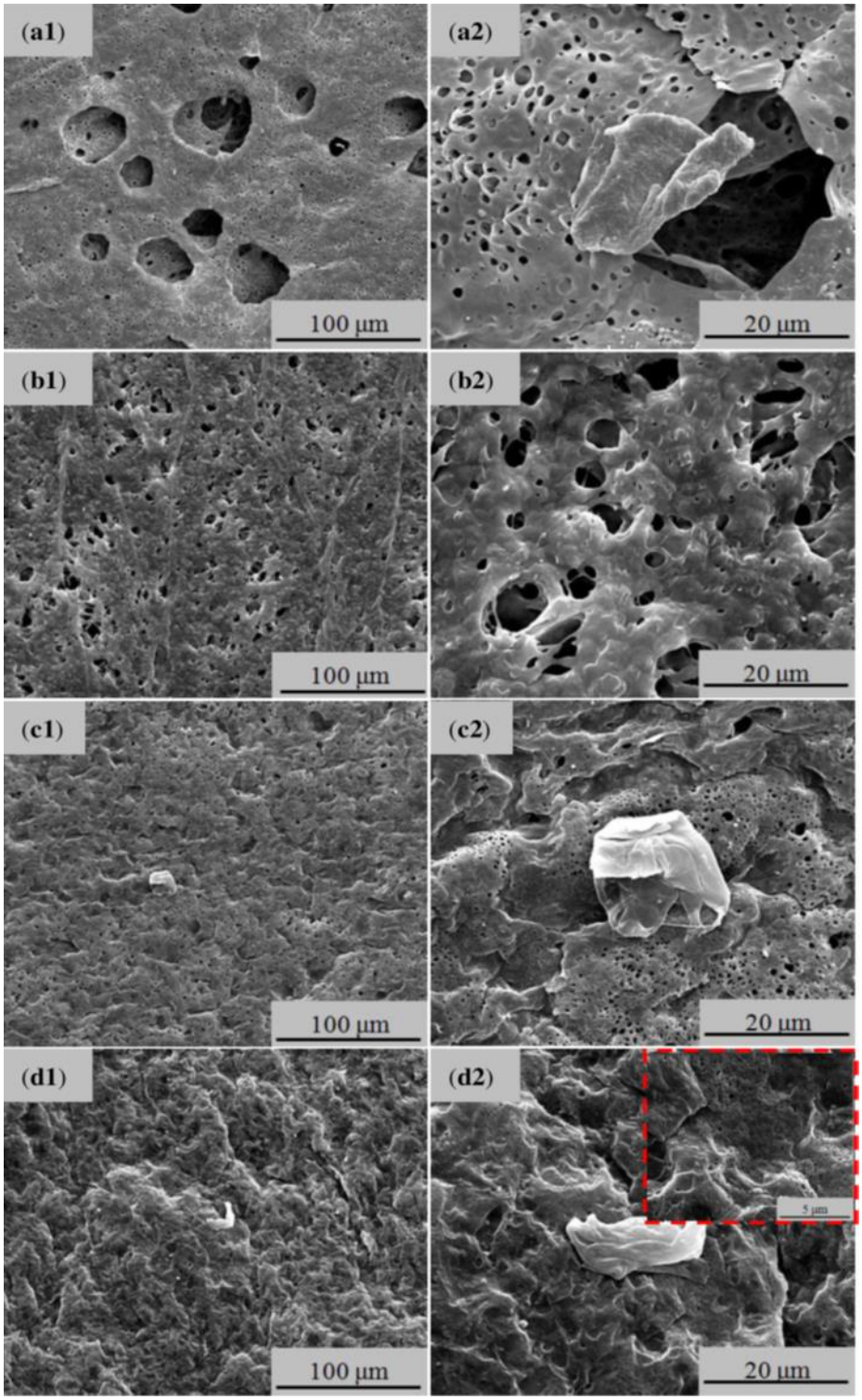

Figure 2.7. SEM images of PVP /PVDF/GO top surface membranes at different GO amount added. (a-1, a-2) 0.2 wt%, (b-1, b-2) 0.5 wt%, (c-1, c-2) 1.0 wt% and (d-1, d-2) 2.0 wt%. [37].

2.4 Adhesion improvement of GO with polymeric substrates

Positively charged polyelectrolytes and membrane surface functionalization were incorporated in many types of research to improve the adhesion between the GO layers and the underlying polymeric membrane supports. **Table** 2.1 shows the chemicals that have been used to stabilize GO on membrane surfaces**. Zhao et al.** [66] developed a uniform reduced graphene oxide (RGO) film on polyethylene terephthalate (PET) substrates using a simple drop-casting method after functionalizing the surface by polydopamine. **Goh et al.** [67] in their research used Polyethyleneimine (PEI) to immobilize GO layers with the hollow fiber poly(amide-imide) surface via dip coating technique.

Hu & Mi. [69] used 1, 3, and 5-benzenetricarbonyl trichloride to cross-link GO nanosheets which were deposited on a Polysulfone membrane support coated by polydopamine to functionalize the surface. The cross-linker provided GO nanosheets an oriented stacking structure that enhanced both the degradation resistance in water and the interlayer spacing between GO layers. **Hegab et al.** [72] fabricated GO functionalized (GO/f-Cs) polyamide membrane for brackish water purification. **Hu and Mi** [70] utilized the electrostatic interaction between negatively charged GO and positively charged polyallylamine hydrochloride (PAH) in fabricating a GO-based membrane on a porous polyacrylonitrile (PAN) membrane. They used the LBL deposition technique to fabricate that particular membrane.

Table 2.1. Chemicals used to stabilize GO on membranes surfaces.

Support	Active layer	Go crosslinker	Technique
Polyacrylonitrile [16]	a hydrolyzed polyacrylonitrile	Poly (ethyleneimine) &polyacrylic acid	LBL & dead end filtration
Polysulfone [14]	PA (polyamide)	amino GO	layer-by-layer (LbL)
Poly(acrylonitrile) [70]	a hydrolyzed polyacrylonitrile	poly(allylamine hydrochloride) (PAH)	(LbL)
Poly-amide [72]		chitosan	
Poly sulfone [69]	poly-dopamine	1,3,5-benzenetricarbonyl trichloride	LbL
Poly(amide-imide) [67]	Poly-ethyleneimine (PEI)	Poly-ethyleneimine (PEI)	dip coating
Poly-(ethylene terephthalate) (pet) [66]	poly-dopamine	---------	simple drop-casting

2.5 Plasma treatment

Plasma is one of the four matter states, which can be formed by either exposing a gas to an intensive electromagnetic field with a microwave generator or by heating the gas to a high temperature. This environment will create positive or negative charged particles (ions) due to the loss or gain of electrons. The plasma is electrically conductive due to the presence large numbers of charged particles so that it can be controlled by electromagnetic fields [81]. Plasma is a highly reactive chemical environment in which several reactions occur.

Mainly, a plasma treatment can refine the polymer surface in many ways, by adjusting some parameters such as the power, the gas stream, the plasma treatment time and the applied vacuum pressure. Etching of the membrane surface, cross-linking and activation takes place during plasma treatment process, as they are all affected by the composition of the gas used during the treatment process and the conditions of the plasma such as fast neutrals, electrons, radicals, and vacuum ultraviolet VUV radiation [82][83]. Surface etching of the polymer mainly takes place due to the interaction of the surface with gas ions or radicals. Although, extra intense treatment may lead to inner chain scissions, which are also supported by VUV radiation[84]. Plasma treatment process conducted for polymeric surfaces causes some surface modification and implants active functional groups at the polymer surface[85].

Using plasma treatment to modify membrane surfaces is an economical and highly efficient technique since it is a quick and simple physical treatment process. In this process, an inert gas such as argon is highly activated to create plasma then accelerated to the substrate. The energy of the plasma ions is conveyed to the atoms of the substrate surface via elastic and inelastic impacts. Some of the substrate surface atoms will gain sufficient energy to escape from the substrate all the way to the vacuum chamber. During this Plasma treatment, the surface will be cleaned of any contaminants, consequently, it is also called plasma cleaning [86].

As mentioned earlier, the membrane surface modification can be achieved by exposing the sample surface to plasma gas. **Laboratories & April** [87] investigated the influence of plasma treatment for polyether sulfone (PES) by O_2, Ar, H_2, Ne, He, and CF_4. In their study, it found that the chemistry and topography of the membrane surface had been

drastically enhanced depending on the gas feed type employed. Moreover, the O_2 plasma treated sample was the most intensively oxidized one while an H_2 plasma treatment caused instantaneous degradation of both sulfur and oxygen from the sample surface. **Steen et al.** [88] also explored the modification of PES membranes by low-temperature H_2O plasma treatment. The water contact angle results confirmed that this type of plasma treatment had improved the wettability of the membrane surface. **Feng et al.** [89] studied the effect of O_2 plasma treatment on PES films and found that oxygen plasma treatment rehabilitated the chemical composition of the surface to a very high degree and increased the surface roughness as shown in **Figure** 2.8**.**

Kim et al. [90] investigated the effect of O_2 plasma treatment on the surface morphology of polysulfone (PS). They found that the water contact angle was decreased by increasing the treatment time and that it became saturated after 20 seconds. Furthermore, the membrane fouling was reduced despite the fact that the water flux was increased. **Wavhal & Fisher** [91] modified ultrafiltration PS membranes by CO_2 plasma treatment and noticed an ultra-enhancement of the membrane water contact angle. The water contact angle decreased to zero and the effect remained even after 3 months. For a polyvinylidene fluoride (PVDF) membrane a radio frequency plasma treatment was conducted by **Kaynak et al.** [92] to improve Polypyrrole adhesion using a mixture of Ar and O2 gasses for the plasma treatment. The abrasion result suggested an acceptable bonding strength between the Polypyrrole and the PVDF surface after plasma treatment. Also, they confirmed an increase in the roughness value for the PVDF surface. Furthermore, the same membrane was modified by using an instantaneous low-temperature plasma and an ammonium carbonate solution by **Zhao et al.** [93]. A

remarkable increase in the surface roughness of the PVDF membrane was observed. They drew the conclusion that this treatment decreases membrane filtration resistance but improves the antifouling property.

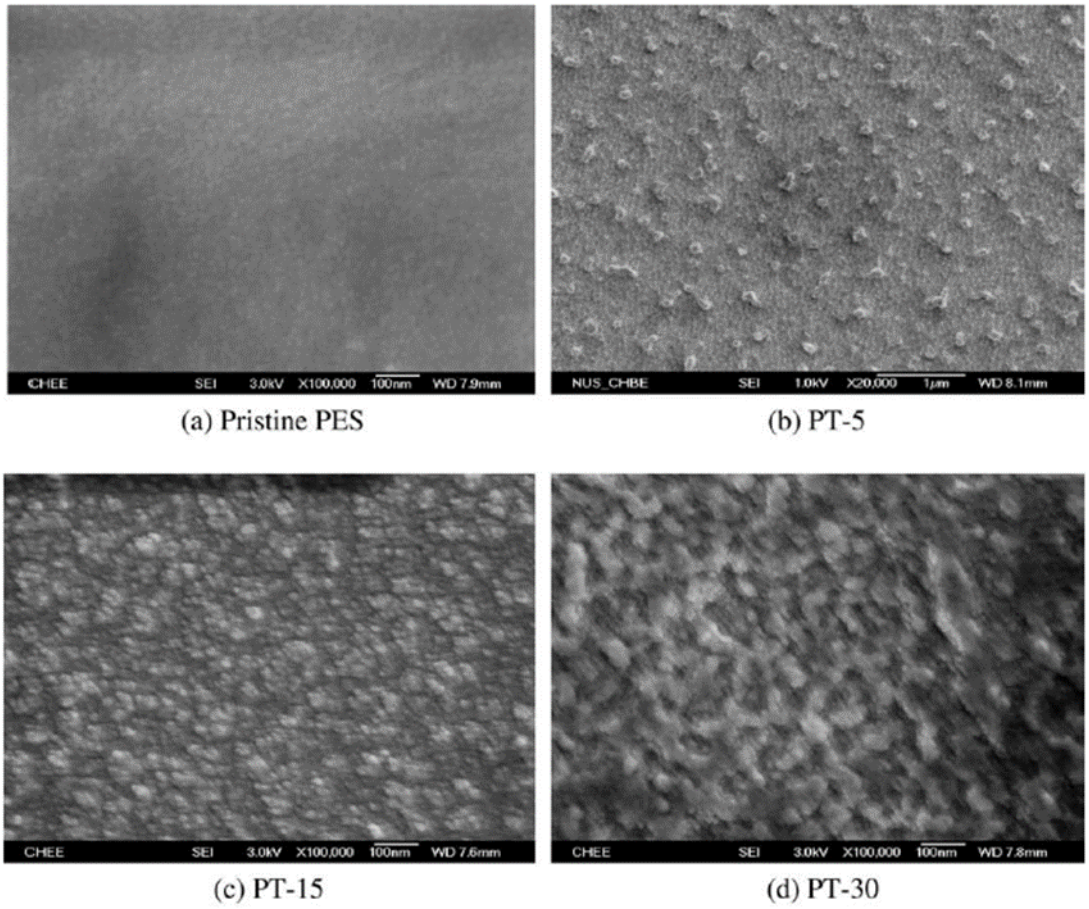

Figure 2.8.SEM images for PES surfaces: (a) before treatment, (b) after 5 min plasma-treatment , (c) after 15 min plasma-treatment, (d) after 30 min plasma-treatment [42]

CHAPTER 3

EXPERIMENTAL WORK

3.1 Materials

A highly-concentrated graphene oxide solution suspension in water (97% water and 3% GO) was used. The range of GO flake size is between 0.5 to 5 microns and it is composed of 79% Carbon, 20% Oxygen and 1% Hydrogen was used in this work and was purchased from Graphene Supermarket (Calverton, New York, USA). A polyether sulfone (PES) ultrafiltration membrane with 30 nm pore was purchased from Sterlitech (Kent, Washington, USA). Hydriodic acid (HI) 55% AR with stabilizer was supplied by Loba Chemie (Wodehouse road, Mumbai, India). Cationic Polyacrylamide (PAM) with M_w = 8-12 Mg/mol was purchased from Polyscience (Warrington, Pennsylvania, USA). Potassium chloride (KCl), used for diffusion studies, was purchased from Merck group chemicals (Germany). Bacteria strain purchased from Scharlau (Barcelona, Spain).

3.2 Substrate preparation

Four 5 cm x 5 cm coupons were cut from the PES membrane sheet. The coupons were washed with deionized water (DI) and prepared for the glow discharge low-pressure air plasma treatment (PT). The coupons were wetted with DI-water before placing inside the plasma treatment chamber (PCD-32G) purchased from Harrick Plasma (Ithaca, New York, USA). Three coupons were plasma treated for 2, 10 and 20min, respectively at 18 W power applied to the radio frequency coil at 8-12 MHz electromagnetic radiation. The

fourth substrate was left as received without plasma treatment and designated as PES-bare for comparison purposes. The same plasma treatment process was repeated for another set of three PES membrane samples to obtain reliable and repeatable results.

3.3 GO and rGO coated PES membrane preparation

A spin coating technique was used to deposit GO layers on PES substrate to fabricate the GO-based membranes. The highly concentrated GO was first diluted with DI-water to obtain a 0.55 mg/ml concentration solution (optimized to give an acceptable GO layer thickness in nanometers). The solution was stirred for 10min to obtain a homogeneous dispersion of GO flakes in DI water. The plasma treated and the PES-bare coupons were cut into 5 cm ×5 cm samples and affixed on a glass slides then mounted on the spinning stage of the spin grower device (Absolute Nano, USA). Recipes for the GO spin coating deposition were optimized and then three GO deposition cycles (deposition-drying-deposition) were repeated for each substrate sample as shown in **Figure** 3.1. One GO deposition cycle consisted of first fixing the spinning speed at 200 rpm and dropping 2 ml of GO solution to achieve in the center of the substrate coupon. the spinning speed at 3000 rpm for a duration of 4 min to exclude excess and weakly bonded GO suspended flakes. A vacuum pump was used to increase the water evaporation rate during the second step while spinning at 3000 rpm. The same deposition procedure was repeated three times for all samples to complete three deposition cycles (3 D.C). In order to make reduced graphene oxide, rGO/PES and GO –PES were exposed to hydriodic (HI) vapor as shown in **Figure** 3.2**.** for 1 hour in a closed flask until the color turned from brown to a

shiny gray indicating that reduced graphene oxide (rGO) film has been obtained in [36][94].

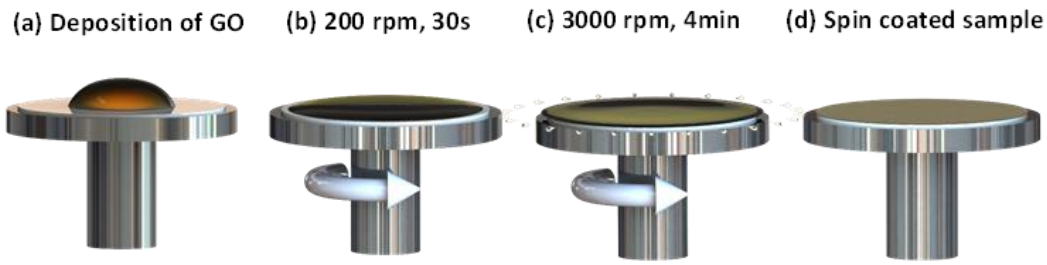

Figure 3.1. Schematic diagram showing spin coating steps of GO layers on substrate surface

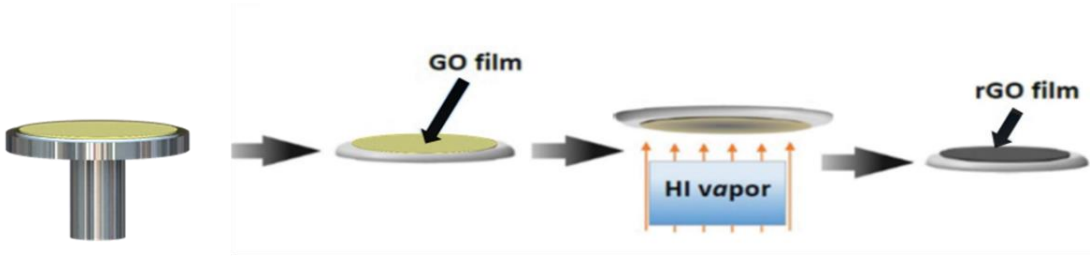

Figure 3.2. GO reduction process via exposure to HI vapor.

3.4 GO/PAM and rGO/PAM coated PES

In order to fabricate GO/PAM coated PES, three samples of PES substrate were cut into 5 cm by 5 cm. The PAM solution was prepared by dissolving 2 grams of PAM powder in 150 ml PH 4 buffer solution and stirred for 2 hours. Then, PES substrate was mounted on the spin grower rotating the disc. Next step was pouring 2 ml of PAM solution at the center of the PES substrate while spinning at 200 rpm for 2 min duration time. This 2 min duration time at low rotating speed to give the PAM enough time to be adsorbed on PES substrate surface. Next step was rotating at 3000 rpm to exclude excess PAM solution. To

remove the weakly bonded PAM layers, the substrate was gently then rinsed with DI-water then spun at 3000 rpm for a duration time of 4 min. In order to add one GO coating layer, 1.5 ml of the GO solution (0.55 mg/ml) was poured into the center of the functionalize PES substrate with PAM following the same procedures used to deposit PAM on the PES. Another GO deposition process was carried out to ensure full coverage of the functionalized surface by GO layers. Another three samples were prepared following the same manner to prepare GO/PAM coated PES with few nanometers thickness (less than 30 nm). The concentration of the GO solution used to prepare these samples was 0.15 mg/ml.

In order to prepare the rGO/PAM coated PES samples, same GO reduction process was performed. The prepared GO/PAM coated PES was subjected to HI vapor for a different time interval (0.5, 2, 6 and 24 hours at 25 ℃ and 0.25, 0.5, 1 and 2 hours at 80 ℃). After each period, part of the prepared membrane with 1 cm by 1cm dimensions was cut out and the remaining membrane was subjected again to the HI vapor to complete the next reduction period. The same procedure was repeated for the other samples to obtain reliable results.

3.5 Characterization of membrane properties

A Bruker Dimension Icon® atomic force microscope AFM was used in tapping mode to examine the surface topography and roughness for all samples. The size of the images was 5 um ×5 um. The average RMS value was calculated out of three different measured values for the same sample at different locations. Water contact angle measurements

(CA) were carried out using an automatic dispenser (Model 500, Ramé-Hart) in order to find out the effect of plasma treatment on substrate surface wettability.

The structure and topography of the coated GO layers were further analyzed by using a field emission scanning electron microscope (FESEM TSCAN-MIRA 3 LM). The surface chemistry of the samples was determined by using a Fourier Transform Infrared Spectroscopy (FTIR) Nicolet 6700 Model (Thermo Scientific).

3.6 Membrane performance evaluation

A diffusion study of KCl ions through prepared membranes was performed in order to evaluate the membrane performance. The diffusion cell used in the experiment was purchased from Permegear (Hellertown, Pennsylvania, USA) and consisted of two 7 ml glass cells with a 3 mm diameter openings. The membrane is sandwiched at the opening between the two cells by water tight clamping of the two parts of the cell as shown in **Figure** 3.3**.** The membrane samples for the diffusion study were one-centimeter diameter pieces which were punched out from the PES and GO/PES samples. Three samples from each membrane were used for the diffusion study.

The two sides of the diffusion cell were first thoroughly washed with a 60% ethanol/DI solution and fully dried. The membrane sample was sandwiched between the two parts of the diffusion cell., One side was filled with Di-water and stirred for 2 min. Then the DI-water was sucked out by syringe and then filled again. This was followed by stirring for 2 min then it was emptied. The same procedure was repeated for the other side with a 0.5 M KCl solution. The next step was filling one side with DI-water and the other side was filled with a 0.5 M KCl solution to begin the diffusion process. Both solutions were

magnetically stirred to minimize the concentration polarization. A conductivity probe supplied by eDAQ (Denistone East, New South Wales, Australia) was dipped in the DI side to measure the conductivity at 1-min intervals for a duration of 10 min. The calibration curve of KCl ions concentration (Mol/L) versus the conductivity values measured by the probe in millisiemens (mS) were plotted and the slope was calculated (Mol/L.mS). This calculated slope value was used to convert the conductivity readings into salt concentration. The diffusion flux of KCl ions (Mol/L.s) passing through the membrane was then calculated after plotting the normalized concentration reading versus the time. The diffusion flux for the PES-bare substrate was considered as a reference for other prepared samples and the percentage of blockage enhancement was calculated according to the following equation:

$$Blockage = \frac{D_s - D_b}{D_b} \times 100\ \%$$

D_b is the diffusion flux for the PES-bare substrate and Ds is the diffusion flux for the prepared sample. For each prepared PES membrane three diffusion tests were carried out, then the average diffusion value was calculated.

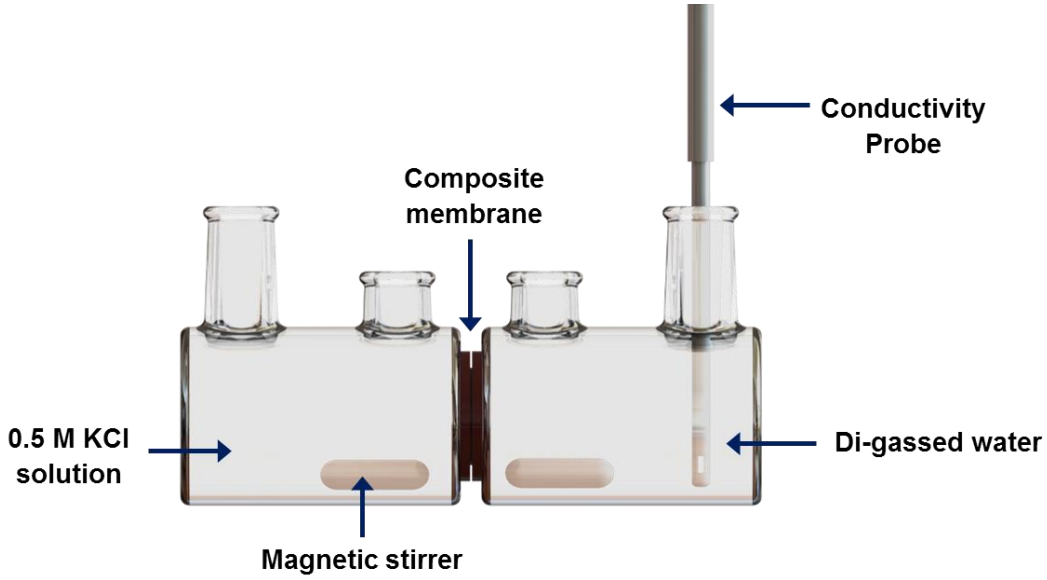

Figure 3.3. Diffusion cell 2D view

3.7 Static bacteria adhesion test

A none-pathogenic bacteria strains were used to evaluate membrane biofouling properties via static bacteria adhesion test. For this test, a non-pathogenic E. coli K12 MG 1655 bacteria strains were used. The Bacteria cells were cultivated overnight in a Tryptone medium at 37 ^{o}C then harvested. A portion of the harvested bacteria was incubated again at the same condition in a fresh Tryptone medium. E. coli bacteria cells were then harvested at 4000 rpm using a centrifugation device for a duration of 10-min and then washed twice at 5 ℃ with a sterile 0.9 % Sodium Chloride solution. A bacteria solution with a concentration of 5 x 108 CFU/mL was then prepared. The prepared bacterial solution was poured into 9 glass test tubes. Three samples of each Bare PES, GO/PES and rGO/PES membranes were cut into 1 cm by 1 cm approximately. The samples were immersed carefully in 10 mL of the prepared bacteria suspension solution (1 x 109

cells/mL). All tubes were then kept inside an incubator for 4 hours at 37 ^{o} C. Each tube was shaken every 30 min to ensure full bacteria exposure along membranes surfaces. To exclude weekly bonded bacteria cells after 4 hours of exposure, a gentle rinsing by a bacteria-free broth media was used. After rinsing process, the samples were dried by exposing them to nitrogen gas flow for 3 min. After that, each membrane sample was mounted on a metallic base then coated by plasma sputtering in order to take SEM images. For each sample, 3 images were taken at a different location then, the average number of the observed counted bacteria was calculated.

CHAPTER 4

RESULTS AND DISCUSSION

4.1 Modification of membrane support

The PES substrate surface was plasma treated to clean and activate the surface to improve the adhesion between the GO layers' and the substrate. The effect of plasma treatment on the PES substrate surface characteristics as a function of treatment time was studied by SEM and AFM images as shown in **Figure** 4.1**.** The SEM images obviously revealed a cleaning effect on the PES substrate surface, which has been treated for 2min. Furthermore, the images showed an enlargement of the membrane surface pores caused by the increase in substrate surface temperature during the prolonged period of plasma treatment [95]. The AFM images revealed an increase in membrane surface roughness as measured by the root mean square roughness (RMS). These results prove that the substrate surface roughness increases with the increase in the Plasma treatment time. This increase in roughness with the increase in plasma treatment time is attributed to the degradation of the PES surface as a result of the ion bombardment during the plasma treatment process [96].

The water contact angle readings (CA) were taken immediately after dropping the water droplet on the sample surface. This upon drop measurement for water CA was performed due to the fact that PES is a hydrophilic membrane and the pore size is relatively large. Consequently, the water droplet will disappear within one second. The CA results

showed slightly enhanced membrane wettability, especially for the 2min PT and 20min PT. This enhancement can be related to the additional oxygenated functional groups introduced onto the PES substrate surface during the plasma treatment process [89].

In contrast, the 10 min plasma treatment process barely affected the substrate surface wettability which can be attributed to the roughness created due to the fine particles observed on the membrane surface in **Figure** 4.1 (c, g) similar to that noticed in the PES-bare. Those fine particles are believed to increase surface roughness which affects the hydrophilicity since the wettability is a compromise between surface roughness and surface free energy or surface functional groups [97]. The cross-section view revealed in **Figure** 4.2**.** proves that plasma treatment has affected the substrate bulk material and the agglomeration indicated by a yellow ellipse is clearly observed, especially for the PES-2min PT sample as compared to the PES-bare substrate. This crosslinking effect is mainly caused by the vacuum ultraviolet VUV radiation [98].

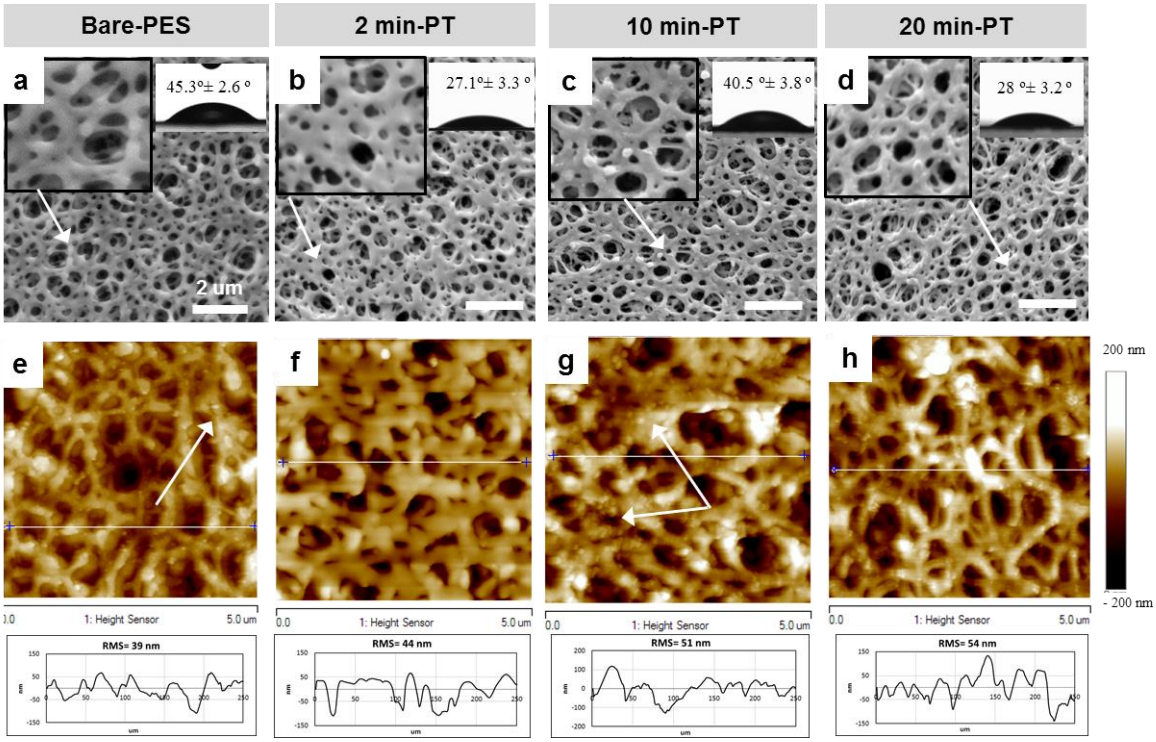

Figure 4.1. SEM and AFM micrographs of (a, e) bare PES, (b, f) 2min PT PES, (c, g) 10min PT PES, (d, f) 20min PT PES.

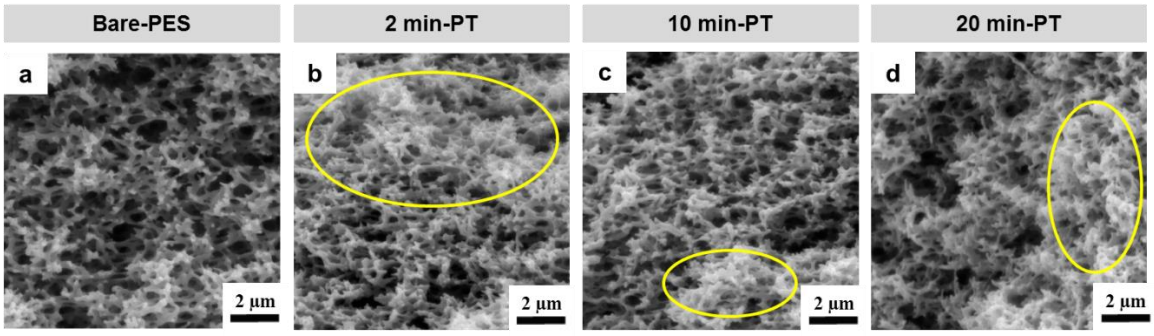

Figure 4.2. SEM cross-sectional view of PES as function of PT time (a) bare PES, (b) 2 min-PT, (c) 10 min, (d) 20 min.

4.2 Characterization of the GO-PES membranes

The GO layers were deposited on PES substrates using spin coating technique as was explained earlier. Different deposition cycles were attempted to achieve full coverage of GO layers on PES with appropriate thickness (between 80-110 nm). **Figure** 4.3 shows cross-sectional images of the developed GO layers on target PES substrates using one

and three deposition cycles respectively. It was found that one deposition cycle yielded GO film of ~50nm thickness, however, three deposition cycles led to ~110nm film thickness. It was found that three deposition cycles achieved full coverage of GO film as compared to one cycle, which exhibited partial coverage of GO layers. Consequently, we utilized three deposition cycles in developing GO/PES membranes as the optimize GO deposition process. After preparing the GO/PES-PT membranes, surface morphology was investigated by SEM as shown in **Figure** 4.3**.** Lower magnification SEM images shown in **Figure** 4.3 (a, b, c, d) proved that three deposition cycles provided a full coverage of GO layers on the PES substrate surfaces. However, higher magnification images for the GO/PES-bare and the GO/PES-PT samples shown in **Figure** 4.3 (e-h) revealed a presence of micro/nano-cracks within the GO layers noticed for the first time. These cracks were observed in all GO/PES samples. Many trials were attempted to avoid the formation of those cracks within the GO layers by changing the PH, the number of deposition cycles, the drying time and the substrate type. None of these trials succeeded in preventing the formation of the cracks as shown in Error! Reference source not found. H owever, an increase in the GO layer thickness did reduce the density of the GO cracks to some extent. It is believed that these cracks developed during the shrinkage of the GO layers after the evaporation of the adsorbed water molecules from the GO layer. This cracking phenomenon of the GO layers is similar to the desiccation cracking of a thin clay soil layers as reported by some researchers [99][100]. It is needless to mention that the presence of these cracks would adversely affect the performance of the GO/PES membranes in blocking the ions transportation.

Furthermore, a cross section image of the developed GO/PES shown in **Figure** 4.5 reveals that the thickness of the spin-coated GO layers on the PES substrate surface was estimated to be around 50 nm for one deposition cycle and 110 nm for three depositions. These results show that the GO spin coated layers' thickness is not linearly related to the number of deposition cycles.

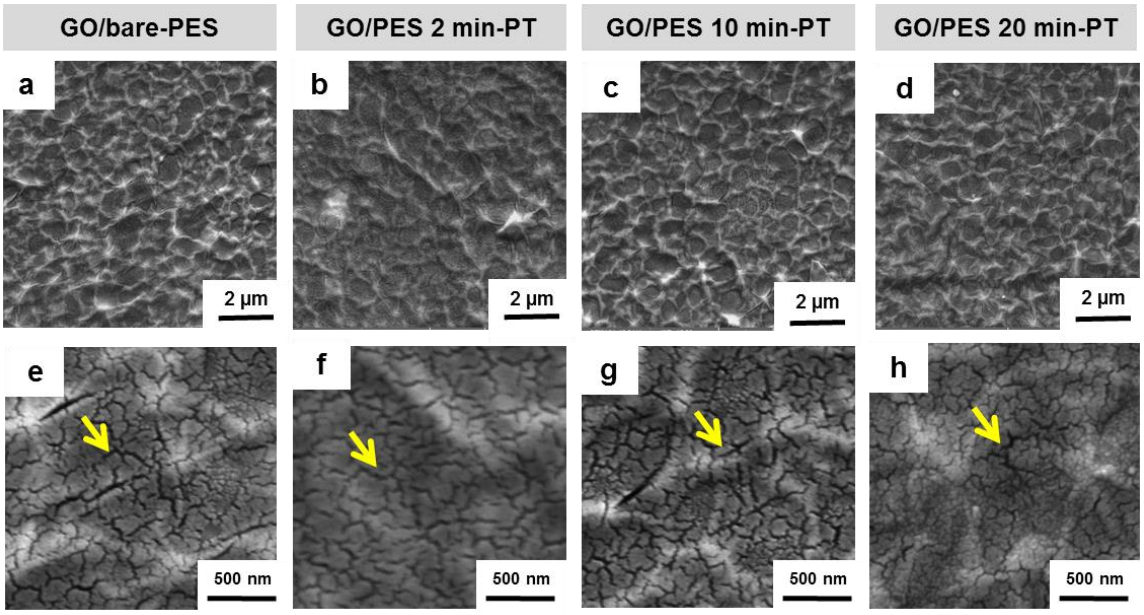

Figure 4.3. FESEM images at low and high magnification for representative parts of fully covered PES substrate surface (a, e), (b, f), (c, g) and (d, h) for O on Bare PES surface and PES PT 2, 10 and 20 min respectively.

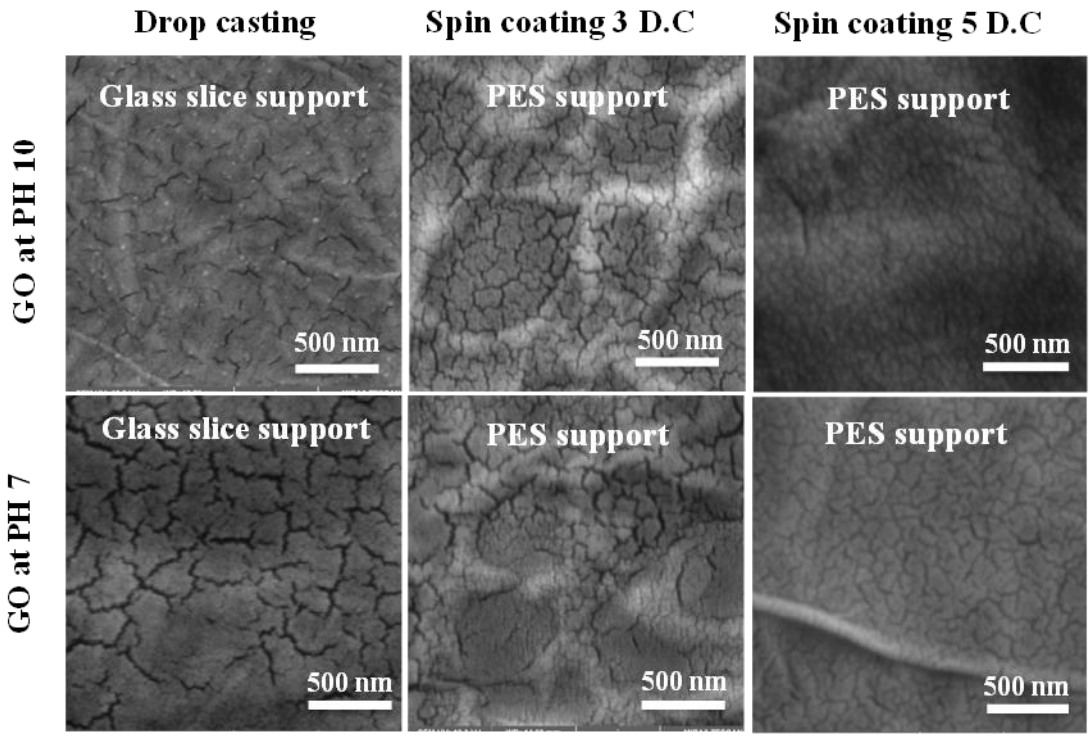

Figure 4.4. High magnification SEM images for GO coated PES and glass slice at different PH values.

.

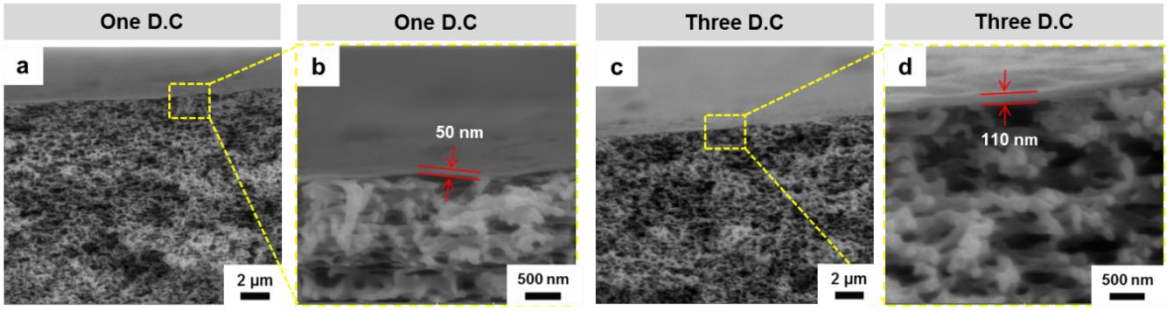

Figure 4.5. Cross-sectional SEM image of GO/PES membrane. (a, b) for one coating deposition cycle, (c, d) three coating deposition cycles at different magnifications.

4.3 Diffusion study results for the GO/PES membrane

A diffusion study was conducted on the plasma treated PES samples to investigate the effect of plasma treatment process on the inner pore structure of the membrane. As

mentioned before, KCl diffusion rate for the PES-bare substrate was used as a reference value. Thus, the ions blockage percentage for the PES-bare PES membrane was considered as a zero percent as shown in **Figure** 4.6. It was found that after the 2-min plasma treatment the KCl ions blockage was increased to 24% as compared to the PES-bare membrane. However, an increase in plasma treatment time to 10 min reduced the blockage percentage to 4%. Further treatment of PES by plasma for 20min again increased the ions blockage to 11%. These results indicate that plasma treatment process has a pronounced effect, not only on the surface but, also on the pore structure. This effect can be related to the relatively large pores and the open structure of PES which allows the plasma treatment to affect the inner structure.

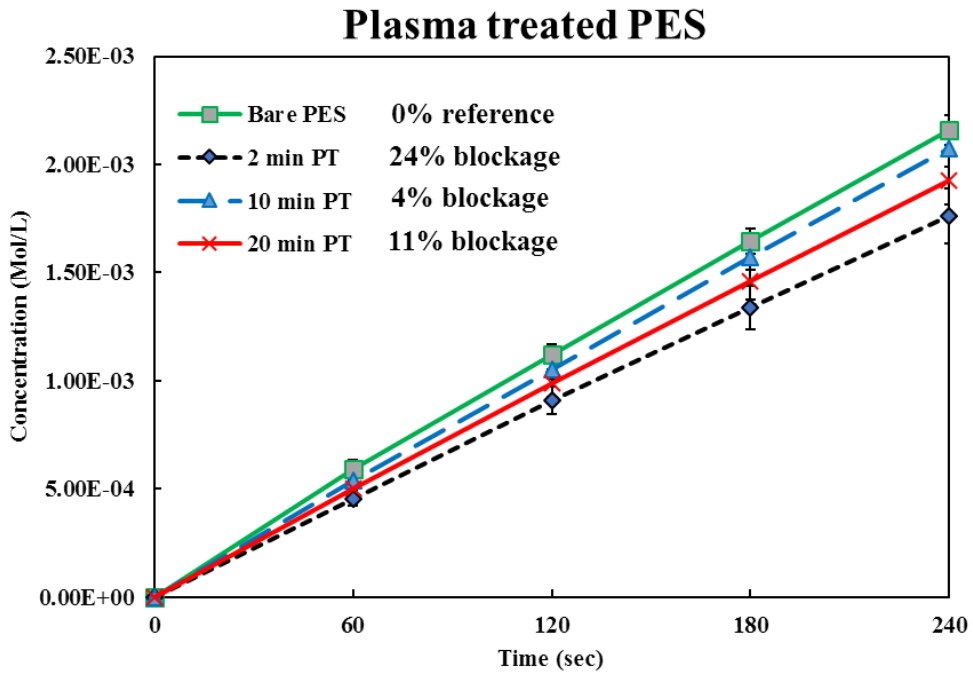

Figure 4.6. Diffusion study results for bare and plasma treated PES for 2, 10 and 20 min.

The above diffusion studies were repeated for the GO/PES-PT samples and the results are shown in **Figure** 4.7**.** It is seen that the addition of GO coating layers enhanced

significantly the KCl ions blockage. Among all the GO/PES plasma treated samples, the GO/PES-2min PT and 20min PT samples yielded the highest blocking value corresponding to 57% and 56% respectively. In contrast, the GO/PES-bare membrane and the GO/PES-10min PT sample exhibited relatively low blocking values for KCl ions when compared to the GO/PES-2min PT and 20min PT samples. The comparison between the plasma treated PES and the GO/PES-PT samples in regards to their KCl ions blocking enhancement is summarized in **Figure** 4.8**.** Moreover, the diffusion rate of KCl ions through the prepared GO/PES-PT membranes is summarized in **Table** 4.1**.**

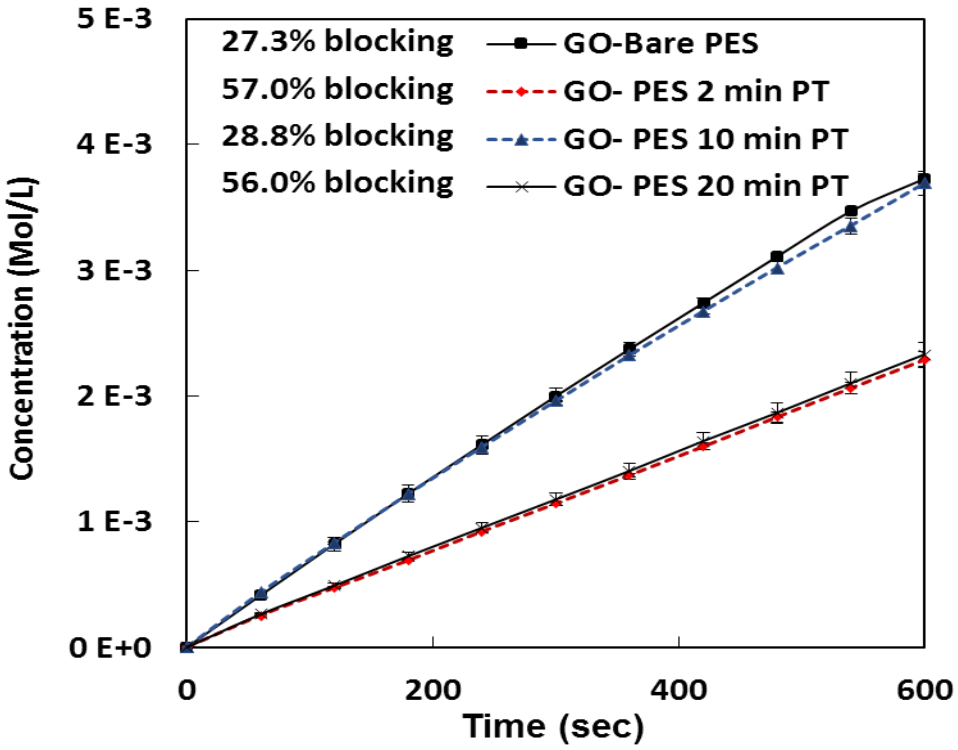

Figure 4.7. Diffusion study results of KCl ions through GO/PES-PT samples.

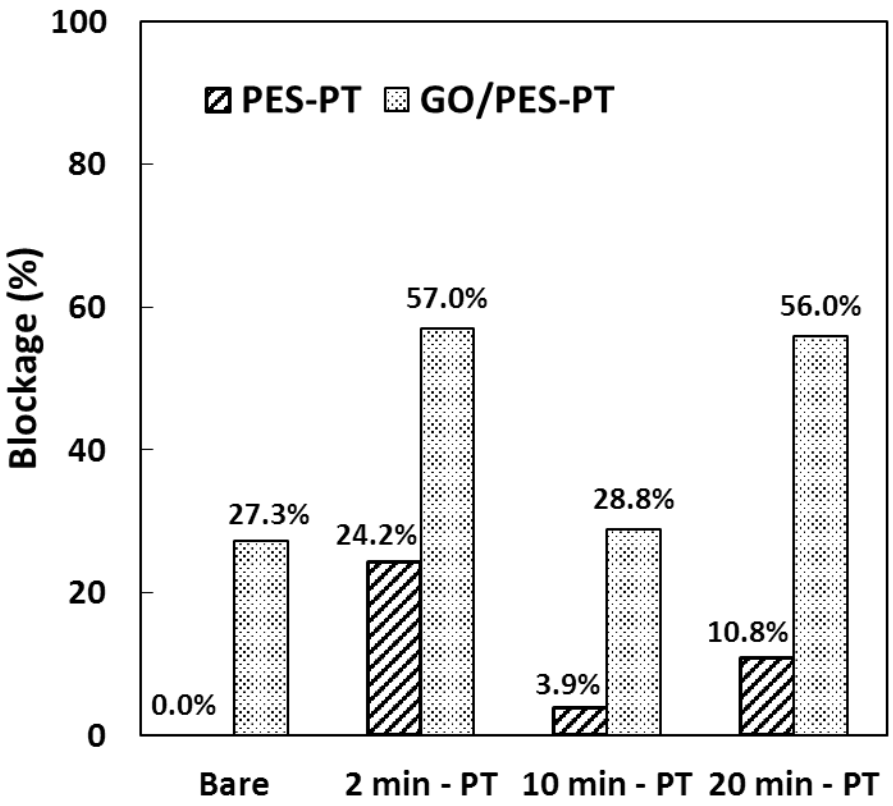

Figure 4.8. Blockage percentage of KCl ions through PT PES and GO PES samples.

Table 4.1. The diffusion rate of KCl salt ions through prepared membranes.

Type	Diffusion rate	Blockage
	Mol/L.s.m²	%
GO/PES-bare	6.45E-06	27.3
GO/PES-2 min PT	3.82E-06	57.0
GO/PES-10 min PT	6.31E-06	28.8
GO/PES-20 min PT	3.90E-06	56.0

In order to understand the previous results, the surface structure of the GO/PES-PT samples was characterized after the diffusion study experiment by SEM as shown in **Figure** 4.9**.** It is seen that the deposited GO layer was partially detached from the PES-

bare and the GO/PES-10min PT sample (**Figure** 4.9(a, c)). However, the GO/PES-2min PT and 20min PT samples exhibited full coverage and a strong attachment of GO layers to the substrate with no evidence of having any detached flakes. Furthermore, higher magnification images **Figure** 4.9 (i, g, k, l)) reveal clearly the detachment of GO flakes and presence of the previously observed cracks. It is believed that both detached flakes and presence of cracks within GO flakes affected KCl ions blockage, since the PES-bare and the GO/PES-10min PT samples gave a lower blockage percentage of around 28% as compared to the GO/PES-2min PT and 20min PT samples, which gave a blockage of about 57%. The above results confirm that the 2min PT and 20min PT effectively enhanced the adhesion between the GO layers and the underlying PES substrate surface even though all the GO/PES samples exhibited uniform cracks on the GO flakes.

The FTIR results for the PES-bare and the GO/PES-2min PT show that a –OH stretch of between 3000 cm^{-1} and 3700 cm^{-1} is clearly observed and the intensity of carbon-containing functional groups C=O and C=C at 1728 cm^{-1} and 1627 cm^{-1} respectively have been increased. These peaks are related to the GO deposited layers. The plasma treatment process conducted for the PES substrate is known to noticeably enhance the oxygen functional groups on the surface since many oxygenated functional groups and polar species are grafted onto the substrate surface [101]. Moreover, the proportions of various components on the surfaces of the PES films such as –O-H, C=C, C-O-C, should increase after plasma treatment as proven by other researchers [89]. These results explain the improved adhesion properties for the GO/PES-2min PT and 20min PT samples since the covalent bond between oxygenated functional groups incorporated on the substrate

surface by the plasma treatment and the GO functional groups are believed to play an important role.

In order to improve the KCl ions blockage percentage, the prepared GO/PES-2min PT sample was then reduced to rGO. The prepared GO/PES-PT was subjected to HI vapor for 1 hour to convert the GO into rGO [36][94]. Digital photos for the PES, GO/PES, and rGO/PES membranes are shown in **Figure** 4.11**.** The produced rGO/PES membrane was then characterized and tested under the same conditions as discussed previously.

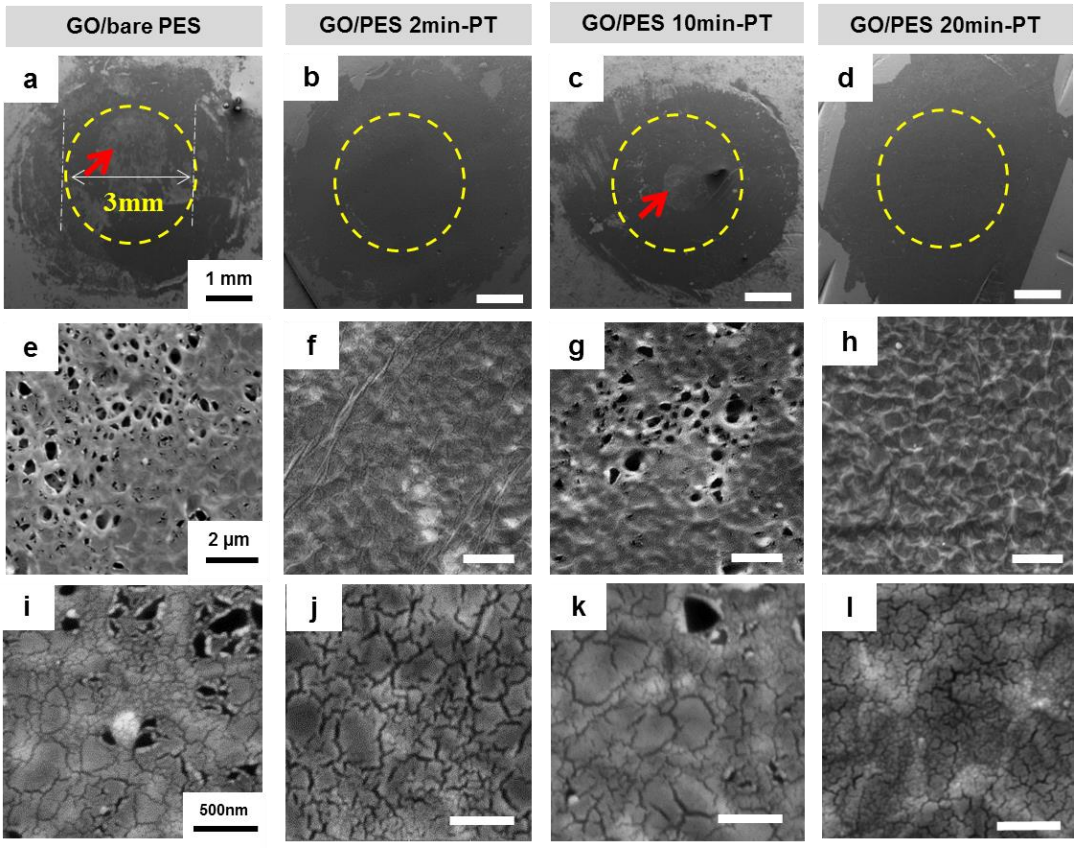

Figure 4.9. SEM images of GO/PES sample on Bare PES surface and PES PT 2, 10 and 20 min respectively. GO detached flakes are indicated by arrows in panels (a, c), where the diameter of active membrane area is about 3 mm. It is clear that 2 and 20 min PT yielded

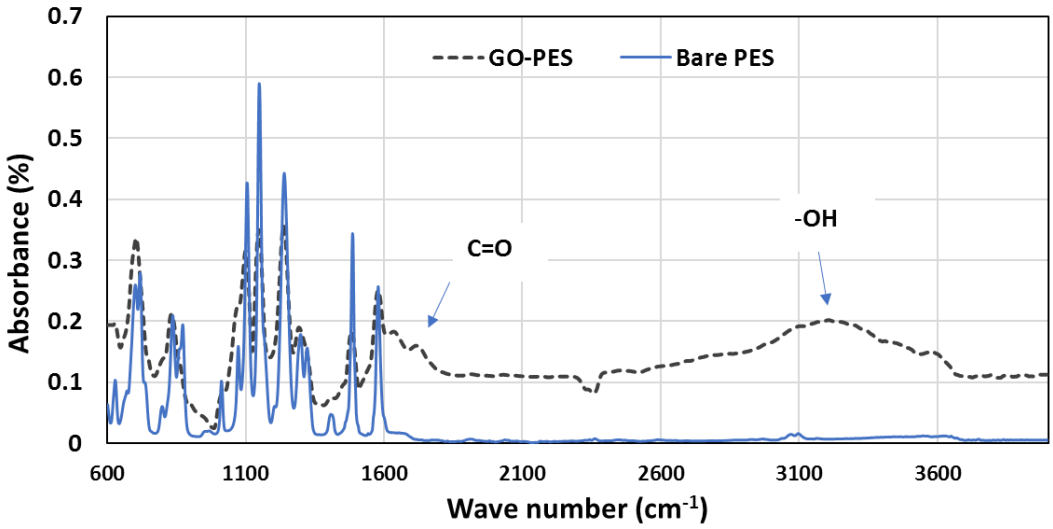

Figure 4.10. FTIR spectra for Bare PES and GO/PES membranes samples respectively.

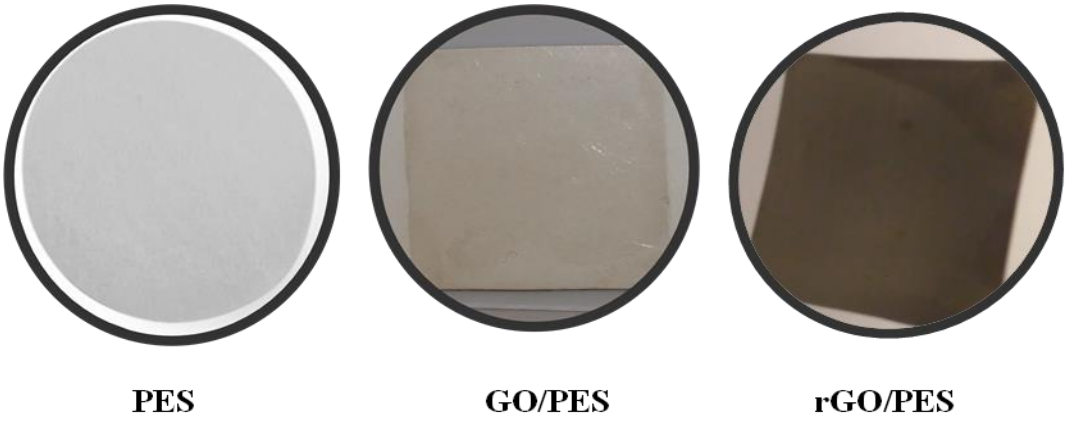

Figure 4.11. Digital photos for PES, GO/PES, and rGO/PES membranes.

The FTIR results are shown in Error! Not a valid bookmark self-reference.(f) proves that the GO layers have been reduced to rGO successfully since the broad O-H stretch between 3000 cm^{-1} to 3700 cm^{-1} in the GO/PES sample was no longer present in the rGO/PES sample. This indicates that the reduction mechanism was mainly a hydroxyl group substitution reaction by a halogen atom [94]. Diffusion study results of KCl ions through the rGO/PES membrane shown in **Figure** 4.12 **(**e) reveal that the KCl ions blockage reached 94% compared to the PES-bare membrane. This significant blocking enhancement for KCl ions through prepared membranes when comparing rGO/PES with

GO/PES samples at the same number of deposited layers can be related to the absence of the cracks in the rGO/PES-2min PT sample as revealed in **Figure** 4.12 (a-d) along with improved mechanical sieving.

The absence of nano-cracks within the rGO sample is believed to be related to the reduced amount of adsorbed water molecules within the rGO layer since the hydroxyl groups in rGO are much lower than in GO. In addition, it is known that oxygen functional groups present in the GO structure are responsible for larger interlayer spacing and it has been proven by other researchers that the oxygen/carbon (O/C) value for GO layers decreases after the reduction process [94][102][103]. Therefore, the mechanical sieving for KCl ions was improved after the GO reduction since the interlayer spacing between the rGO layers decreased. Since rGO was shown to give a high KCl ions blockage percentage we prepared additional rGO/PES-2min PT with 1 and 5 deposition cycles (D.C) of the rGO. The same diffusion study previously discussed was utilized to investigate the effect GO deposition cycles on the membrane performance. The diffusion study results as well as the water permeation results through the prepared membranes at 10 bar are shown in **Figure** 4.13**.** Furthermore**,** the diffusion rate of KCl ions through the prepared rGO membranes are summarized in **Table** 4.2**.** As it was expected, increasing the rGO layers will reduce both salt ions diffusion rate and water permeability as a result of the prolonged water passage and vice versa. For one D.C. of the rGO deposited on PES-2min PT sample, the KCl rejection and water permeation were 92.2% and 133.7 L/m^2.hr, however, for 5 D.C. the rejection reached a 99.3% enhancement with a water permeation flux of 26.7 L/m^2 hr.

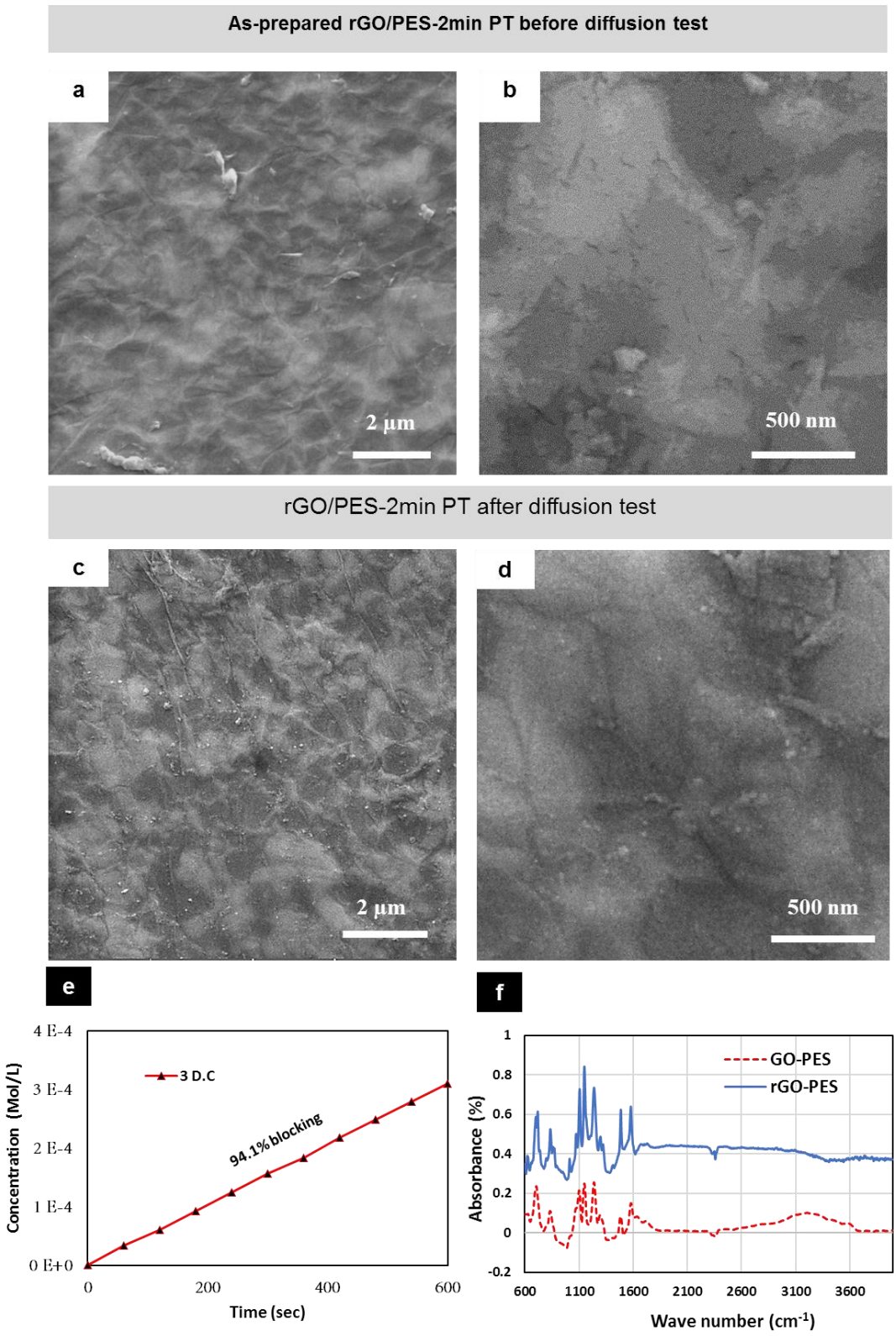

Figure 4.12. FESEM of rGO coated 2min PT PES membrane surface (a, b) and (c, d) at different magnifications before and after the diffusion test, (e) is the diffusion study result for the sample before the diffusion and (f) is FTIR result for the same sample.

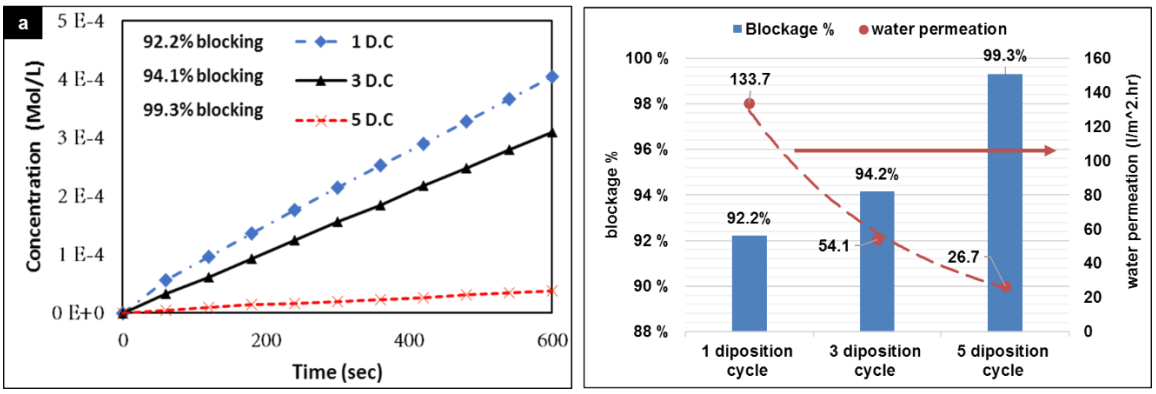

Figure 4.13. (a) Diffusion study results for 1, 3 and 5 deposition cycles (D.C) of rGO on PES 2 min PT (b) DI-water permeation through the membranes at 10 bar.

Table 4.2. The diffusion rate of KCL ions through prepared 1, 3 and 5 D.C rGO/PES membranes.

Type	Diffusion rate	Blockage
	Mol/L.s.m2	%
1 deposition cycle	6.90E-07	92.2
3 deposition cycles	5.18E-07	94.2
5 deposition cycles	6.30E-08	99.3

4.4 Diffusion study results for the rGO/PAM coated PES membrane

Two different concentrations for the GO solution (0.15 mg/ml and 0.55 mg/ml) were used to prepare samples with two different thicknesses. In order to estimate the thickness of the prepared membranes, SEM images were taken for the membranes cross-section as shown in **Figure** 4.14**.**

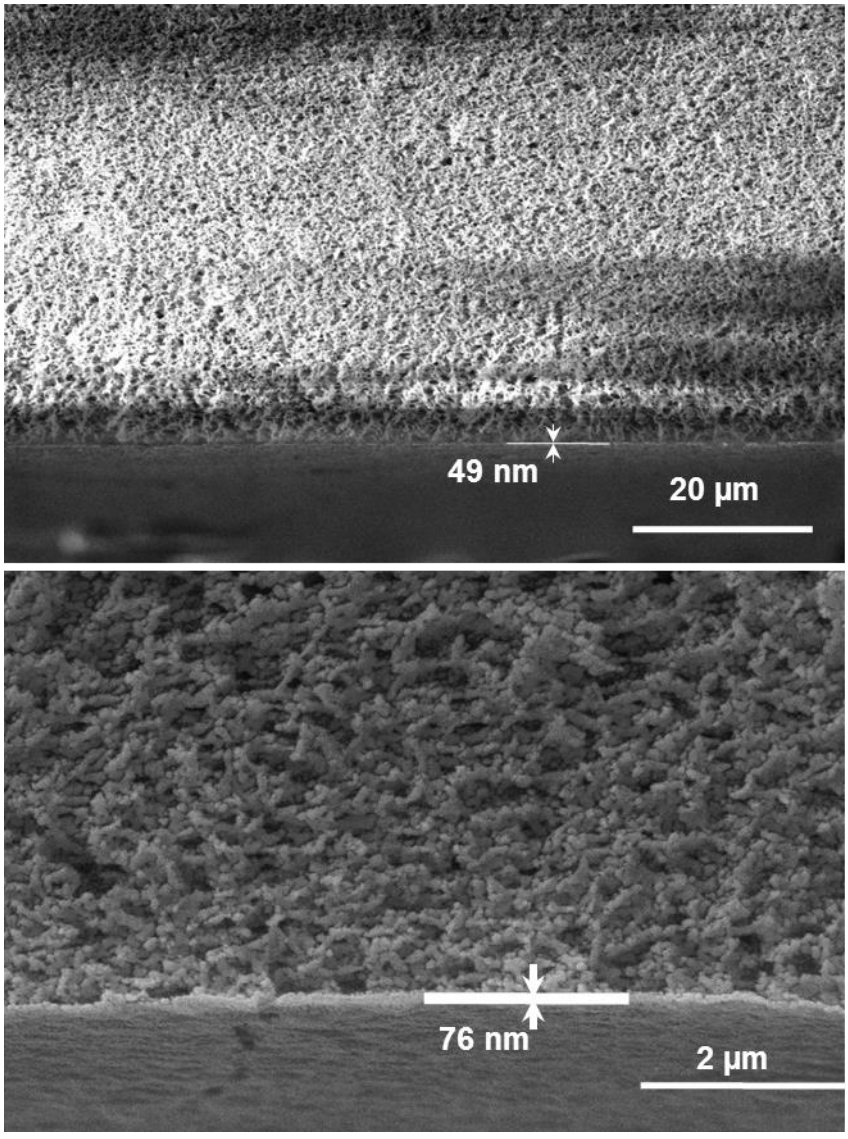

Figure 4.14. SEM images showing the cross-section view of the rGO/PAM coated PES for (a) 2H sample and (b) 2L sample.

The approximate thickness of the membranes prepared using GO solution with 0.55 mg/ml (referred as a 2H sample) was 76 nm on average and the one prepared using GO with 0.15 mg/ml (referred as 2L samples) was 49 nm on average.

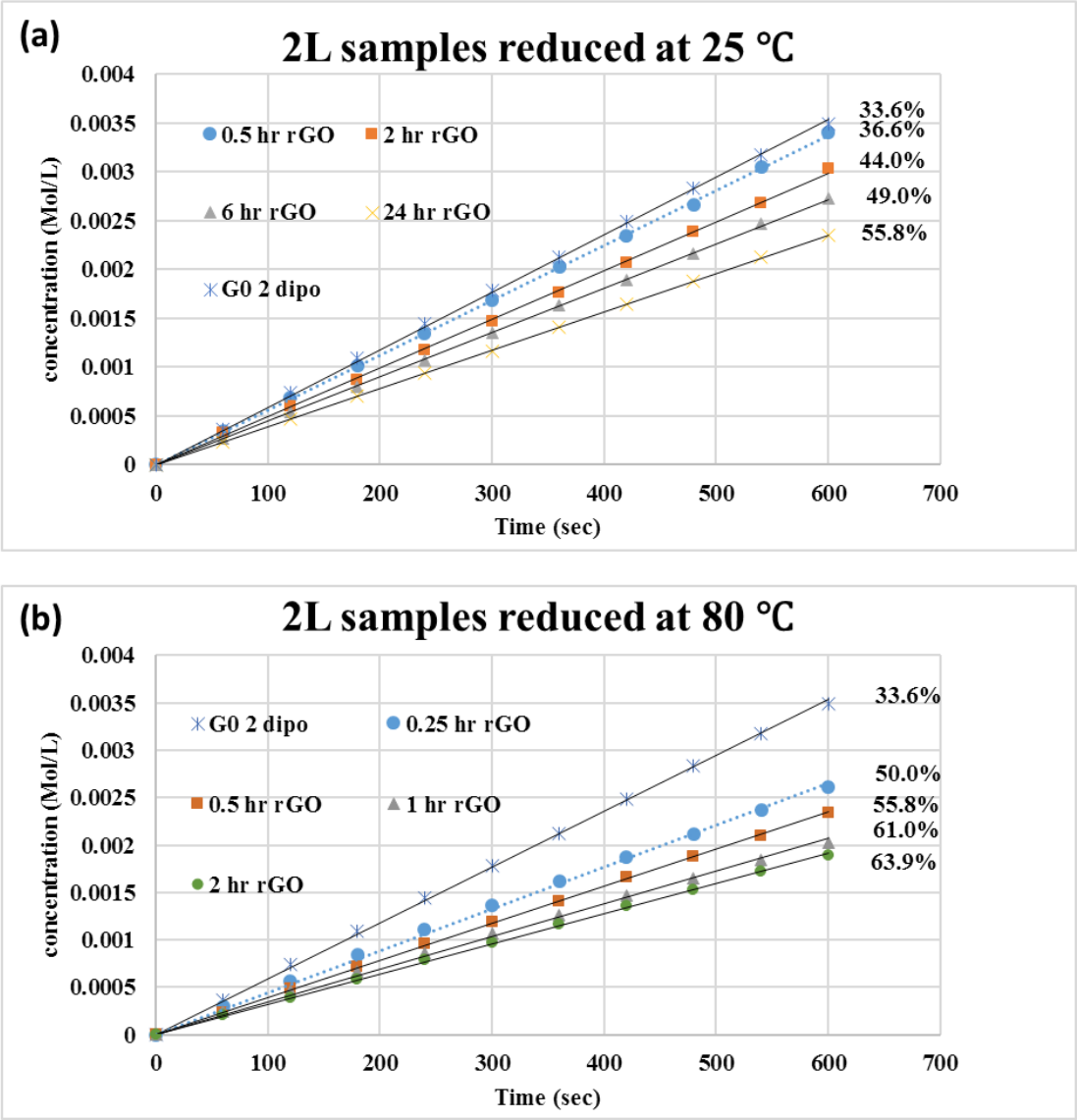

Figure 4.15. Diffusion study results of the KCl ions passing through the prepared 2L rGO/PAM-PES samples (a) at 25 ℃ HI solution and (b) at 80 ℃ HI solution.

A diffusion study for KCl ions transporting through the prepared rGO/PAM coated PES membranes was performed to comprehend the effect of the reduction time (HI vapor exposure period) on the membrane separation performance. **Figure** 4.15. shows the

diffusion study results of the KCl ions passing through the prepared 2L samples reduced for a different duration time at 25℃ and 80 ℃. It was clearly observed that GO reduction for 2-hr by HI vapor maintained at 80 ℃ is giving better KCl ions rejection when compared to the same sample reduced by HI vapor maintained at 25℃.

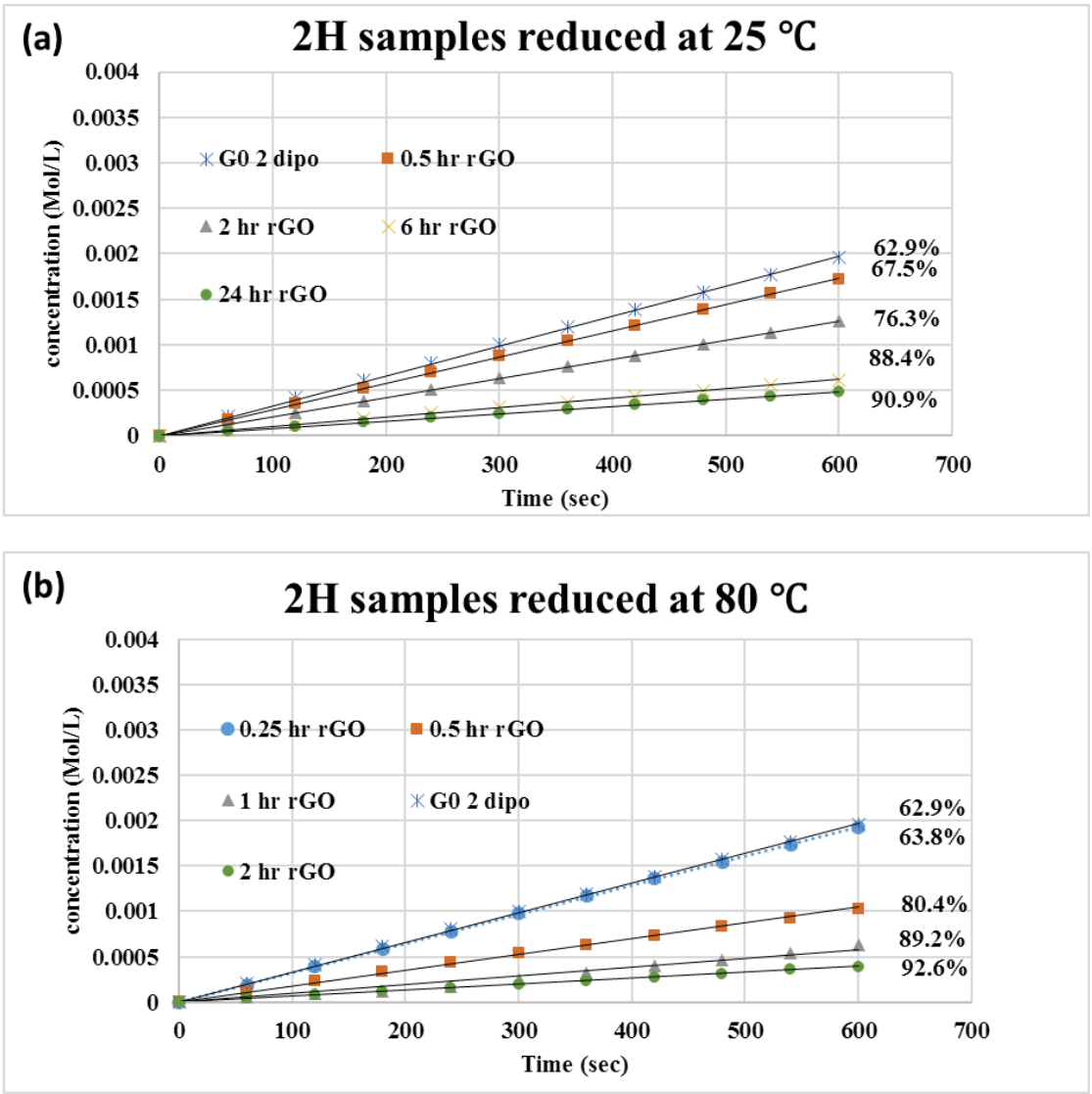

Figure 4.16. Diffusion study results of the KCl ions passing through 2H rGO/PAM-PES samples (a) at 25 ℃ HI solution and (b) at 80 ℃ HI solution.

Figure 4.16. shows the diffusion study results of the KCl ions passing through the prepared 2H samples reduced for a different time duration at 25℃ and 80 ℃. As it was

expected, the same rejection behavior of the 2L samples has been noticed for the 2H samples. The comparison between 2L and 2H samples regarding KCl ions rejection percentage at the same HI solution temperature is illustrated in **Figure** 4.17**.** The results showed that as the reduction time and GO layers' thickness increase, KCl ions blockage increase. Furthermore, raising HI solution temperature increases GO reduction rate since it increases the amount of the HI vapor subjected to the surface of the samples.

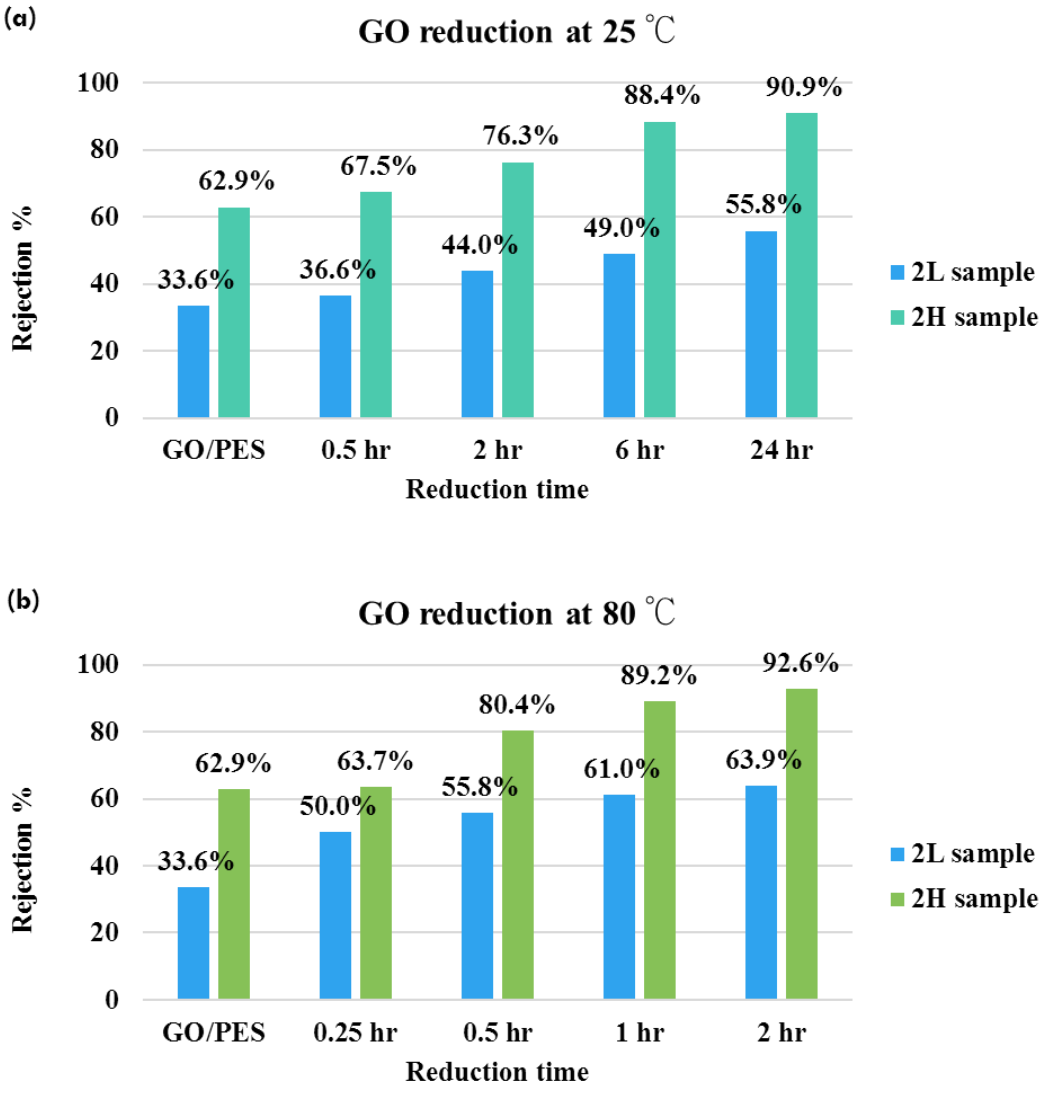

Figure 4.17. KCl ions rejection percentage results as a comparison between 2L and 2H samples reduced by HI vapor while HI solution was maintained (a) at 25 ℃ and (b) at 80℃.

A permeation test was utilized at 10 bar to investigate the reduction time effect on the permeated water flux and the results are shown in **Figure** 4.18. It is clearly noticed that as the reduction time increases, the permeated water flux decreases. However, the sample reduced for 2 hour showed a permeation flux higher than the sample reduced for 1 hour. This can be attributed to the rGO brittleness and the tendency of the rGO to crack under high water pressure.

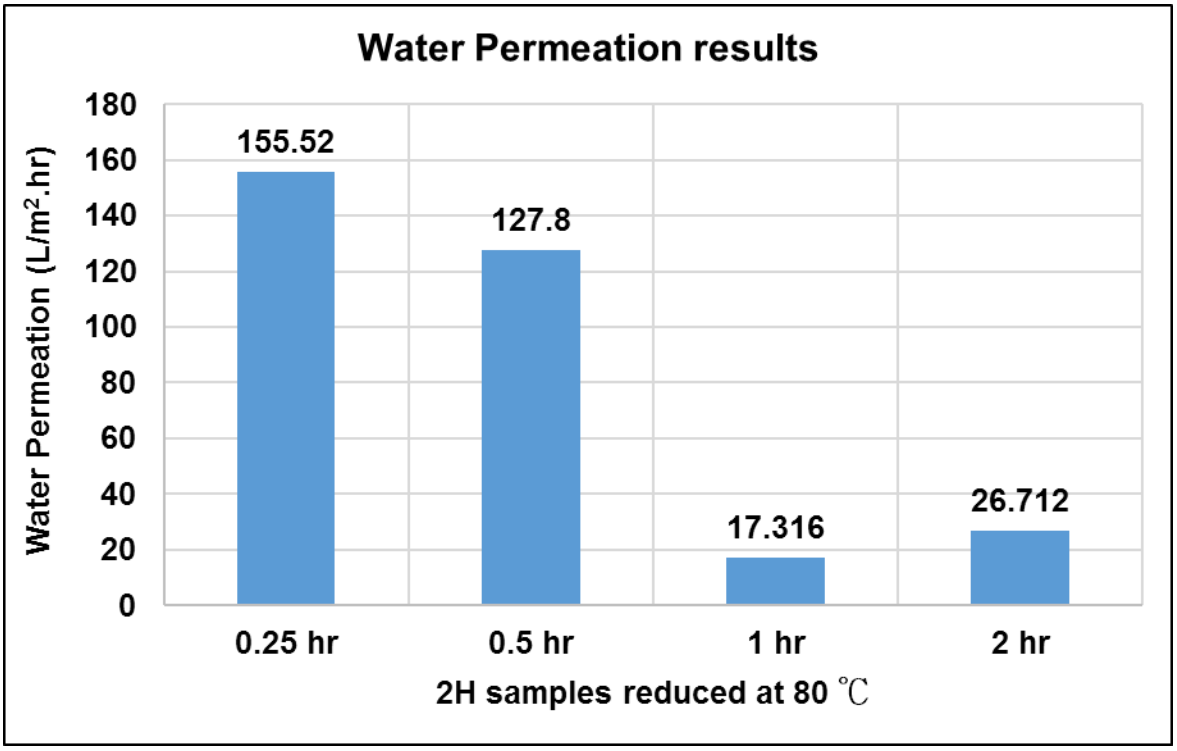

Figure 4.18. The permeated water flux through 2H samples reduced at 80 ℃ for different time intervals.

4.5 Static bacteria adhesion test results

This test was performed to study the anti-bacterial properties of the prepared GO/PAM and rGO/PAM coated PES membrane. The effect of the reduction time on the short-term E. coli adhesion was investigated. In order to perform these tests, the prepared GO and rGO/PAM coated PES samples were exposed to the E. coli suspension for 3 hours. A SEM images were then captured at 3000 magnifications to deduce the relative bacteria adhesion by counting the average number of attached bacteria over the scanned area. **Figure** 4.19. shows the SEM images of the exposed samples to the E. coli bacteria strain solution along with the water contact angle.

Generally, all samples exhibited few numbers of individual bacteria cells attached to the surface of each sample. Moreover, Recent studies have suggested that the GO inactivates the bacteria by physical disruption after direct contact [104], oxidation and charge transfer [105] and lipid removal from the cell[106]. As a comparison between all the prepared sample, the rGO/PAM -PES reduced for 0.25 hour exhibited the highest water contact angle and the highest bacterial intensity. This can be explained by the fact that hydrophilic membrane surfaces form and maintain a thin film of water that can act as a barrier work toward weakening bacteria adhesion to the membrane surface in contrast to the hydrophobic one.

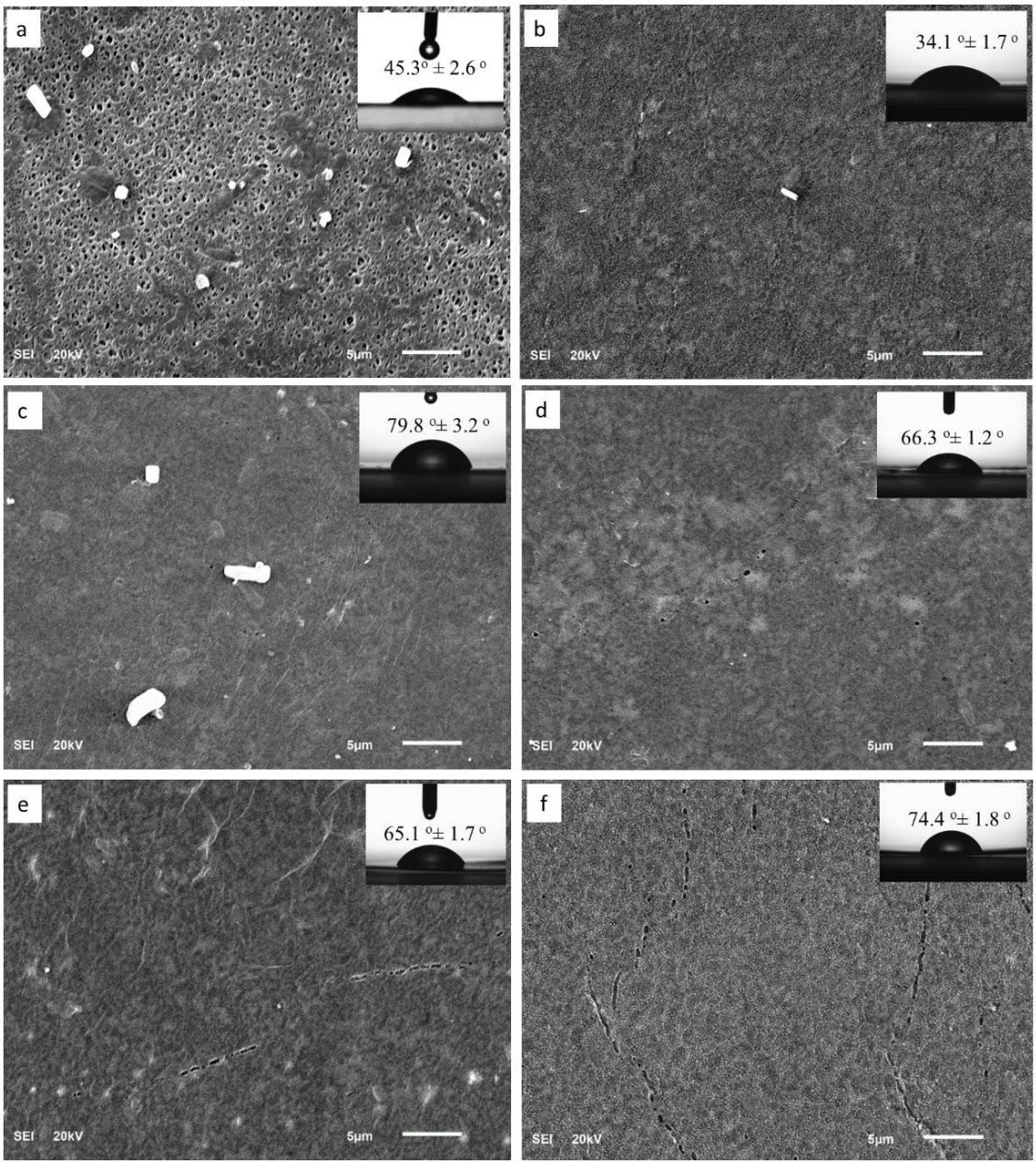

Figure 4.19. SEM image of a representative surface area after 3 hours' immersion in the bacteria solution for (a) Bare PES, (b) GO/PAM-PES, (c) 2H reduced for 0.25-hr, (d) 2H reduced for 0.5-hr, (e) 2H reduced for 1-hr and (f) 2H reduced for 2-hr.

CHAPTER 5

CONCLUSIONS AND RECOMMENDATIONS

5.1 Conclusions

The effect of plasma treatment (PT) on the adhesion of GO/rGO with PES substrate and its subsequent impact on the GO/rGO-PES membrane performance was demonstrated in detail. The results showed that plasma treatment influenced the surface morphology, pore structure, and hydrophilicity of PES-treated substrates. The 2-min plasma treatment and 20-min plasma treatment showed a significant decrease in contact angle values as compared to the non-treated PES substrate. This confirmed that the PES surface became more hydrophilic by plasma treatment. This improved wettability and consequently promoted better adhesion of GO flakes on PES substrate as compared to non-treated PES. Plasma treatment also affected the internal pore structure, since it decreased the average pore size of the plasma treated PES samples as evidenced by the SEM cross-section images and the increase in KCl ion blockage (~28% on average) of the PES-PT membrane as compared to PES-bare membrane.

Although the synthesized GO/PES-PT membranes showed enhanced KCl ion blockage of about 57% in particularly for 2-min and 20-min plasma treatment, the presence of high density of micro/nano-cracks within deposited GO layers rendered them non-usable due to their low salt rejection. The origin of these cracks was likely related to the evaporation of adsorbed water molecules of GO layers during the drying process.

The use of rGO instead of GO, however, exhibited significant improvement in KCl ion blockage of about (94% and 99% for 3 and 5 D.C respectively) as compared to the PES-bare membrane. The permeation resuts through the rGO coated PES proved that as the number of the rGO D.C increases, the water permeation flux decreases. The micro/nano-cracks were absent in the rGO/PES membranes. The absence of cracks in rGO/PES-PT membranes could be attributed to the reduced amount of the adsorbed water molecules into rGO due to the removal of hydroxyl groups after reduction of GO flakes. This also enabled the formation of narrower interlayer spacing between rGO layers, which was beneficial for improving mechanical sieving of the developed membrane.

The use of positively charged polyacrylamide (PAM) as an adhesive layer by spin coating PAM on PES membrane surface had further improved GO and rGO stability on PES membrane surface. The anti-bacterial properties and reduction time effect on the selectivity of the prepared GO/PAM and rGO/PAM coated PES was also investigated. The results proved that All GO/PAM and rGO/PAM coated PES sample exhibited good antibacterial properties. Moreover, it was clearly observed that, as GO reduction time and GO layers' thickness increased, KCl ions blockage increased and the permeated water flux decreased.

5.2 Recommendations

Based on the fabricated membranes results, the following recommendations are suggested for future study:

- Study of the prepared rGO/PAM-PES membranes reduced for 1 hour under cross flow conditions.

- Investigate the performance of the prepared membranes regarding heavy metal removal.
- Investigate the Chemical Resistance Properties of the fabricated GO/PAM and rGO/PAM coated PES membranes.

References

[1] B. S. Lalia, V. Kochkodan, R. Hashaikeh, and N. Hilal, "A review on membrane fabrication: Structure, properties and performance relationship," *Desalination*, vol. 326, pp. 77–95, 2013.

[2] M. FREEMANTLE, "MEMBRANES FOR GAS SEPARATION," *Chem. Eng. News*, vol. 83, no. 40, pp. 49–57, Oct. 2005.

[3] *Advanced Membrane Technology and Applications*. 1016.

[4] M. Elimelech and W. A. Phillip, "The future of seawater desalination: energy, technology, and the environment.," *Science*, vol. 333, no. 6043, pp. 712–7, Aug. 2011.

[5] H. Li, Z. Song, X. Zhang, Y. Huang, S. Li, Y. Mao, H. J. Ploehn, Y. Bao, and M. Yu, "Ultrathin, Molecular-Sieving Graphene Oxide Membranes for Selective Hydrogen Separation," *Science (80-.).*, vol. 342, no. 6154, pp. 95–98, Oct. 2013.

[6] C. Lee, X. Wei, J. W. Kysar, and J. Hone, "Measurement of the elastic properties and intrinsic strength of monolayer graphene.," *Science*, vol. 321, no. 5887, pp. 385–8, Jul. 2008.

[7] D. A. Dikin, S. Stankovich, E. J. Zimney, R. D. Piner, G. H. B. Dommett, G. Evmenenko, S. T. Nguyen, and R. S. Ruoff, "Preparation and characterization of graphene oxide paper.," *Nature*, vol. 448, no. 7152, pp. 457–60, Jul. 2007.

[8] S. Chen, L. Brown, M. Levendorf, W. Cai, S.-Y. Ju, J. Edgeworth, X. Li, C. W. Magnuson, A. Velamakanni, R. D. Piner, J. Kang, J. Park, and R. S. Ruoff, "Oxidation resistance of graphene-coated Cu and Cu/Ni alloy.," *ACS Nano*, vol. 5, no. 2, pp. 1321–7, Feb. 2011.

[9] S. Bano, A. Mahmood, S.-J. Kim, and K.-H. Lee, "Graphene oxide modified polyamide nanofiltration membrane with improved flux and antifouling properties," *J. Mater. Chem. A*, vol. 3, no. 5, pp. 2065–2071, 2015.

[10] A. Altaee, G. Zaragoza, and H. R. van Tonningen, "Comparison between Forward Osmosis-Reverse Osmosis and Reverse Osmosis processes for seawater desalination," *Desalination*, vol. 336, pp. 50–57, 2014.

[11] D. B. Hall, P. Underhill, and J. M. Torkelson, "Spin Coating of Thin and Ultrathin Polymer Films," *Polym. Eng. Sci.*, vol. 38, no. 12, pp. 2039–2045, 1998.

[12] G. M. Shi, J. Zuo, S. H. Tang, S. Wei, and T. S. Chung, "Layer-by-layer (LbL) polyelectrolyte membrane with Nexar^{TM} polymer as a polyanion for pervaporation

dehydration of ethanol," *Sep. Purif. Technol.*, vol. 140, pp. 13–22, 2015.

[13] A. Toutianoush, L. Krasemann, and B. Tieke, "Polyelectrolyte multilayer membranes for pervaporation separation of alcohol/water mixtures," *Colloids Surfaces A Physicochem. Eng. Asp.*, vol. 198, pp. 881–889, 2002.

[14] W. Choi, J. Choi, J. Bang, and J.-H. Lee, "Layer-by-Layer Assembly of Graphene Oxide Nanosheets on Polyamide Membranes for Durable Reverse-Osmosis Applications," *ACS Appl. Mater. Interfaces*, vol. 5, no. 23, pp. 12510–12519, Dec. 2013.

[15] H. K and T. B, "Layer-by-layer assembled membranes containing hexacyclen-hexaacetic acid and polyethyleneimine N-acetic acid and their ion selective permeation behaviour," *J. Memb. Sci.*, vol. 341, no. 1–2, pp. 261–267, 2009.

[16] N. Wang, S. Ji, G. Zhang, J. Li, and L. Wang, "Self-assembly of graphene oxide and polyelectrolyte complex nanohybrid membranes for nanofiltration and pervaporation," *Chem. Eng. J.*, vol. 213, pp. 318–329, 2012.

[17] N. Kotov, S. Magonov, and E. Tropsha, "Layer-by-Layer Self-Assembly of Alumosilicate-Polyelectrolyte Composites," *Chem. Mater.*, vol. 10, no. 3, pp. 886–895, 1998.

[18] P. Stroeve, V. Vasquez, M. A. N. Coelho, and J. F. Rabolt, "Gas transfer in supported films made by molecular self-assembly of ionic polymers," *Thin Solid Films*, vol. 284–285, pp. 708–712, Sep. 1996.

[19] L. Krasemann and B. Tieke, "Selective Ion Transport across Self-Assembled Alternating Multilayers of Cationic and Anionic Polyelectrolytes," *Langmuir*, vol. 16, no. 2, pp. 287–290, Jan. 2000.

[20] L. Shao, J. L. Lutkenhaus, M. H. Kaplan, R. M. Corn, T. Kunitake, M. F. Rubner, R. E. Cohen, P. Schaaf, B. Senger, and F. Boulmedais, "Thermochemical properties of free-standing electrostatic layer-by-layer assemblies containing poly(allylamine hydrochloride) and poly(acrylic acid)," *Soft Matter*, vol. 6, no. 14, p. 3363, 2010.

[21] W. H. Jr and R. Offeman, "Preparation of graphitic oxide," *J. Am. Chem.*, 1958.

[22] H. C. Schniepp, J.-L. Li, M. J. McAllister, H. Sai, M. Herrera-Alonso, D. H. Adamson, R. K. Prud'homme, R. Car, D. A. Saville, and I. A. Aksay, "Functionalized single graphene sheets derived from splitting graphite oxide.," *J. Phys. Chem. B*, vol. 110, no. 17, pp. 8535–9, May 2006.

[23] B. C. Brodie, "On the Atomic Weight of Graphite," *Philos. Trans. R. Soc. London, Vol. 149, pp. 249-259*, vol. 149, pp. 249–259, 1859.

[24] M. Ciszewski, A. Mianowski, G. Nawrat, and P. Szatkowski, "Reduced Graphene Oxide Supported Antimony Species for High-Performance Supercapacitor Electrodes," *ISRN Electrochem.*, vol. 2014, pp. 1–7, 2014.

[25] H. A. Becerril, J. Mao, Z. Liu, R. M. Stoltenberg, Z. Bao, and Y. Chen, "Evaluation of solution-processed reduced graphene oxide films as transparent conductors.," *ACS Nano*, vol. 2, no. 3, pp. 463–70, Mar. 2008.

[26] Z. Liu, Q. Liu, Y. Huang, Y. Ma, S. Yin, X. Zhang, W. Sun, and Y. Chen, "Organic Photovoltaic Devices Based on a Novel Acceptor Material: Graphene," *Adv. Mater.*, vol. 20, no. 20, pp. 3924–3930, Oct. 2008.

[27] D. Li, M. B. Müller, S. Gilje, R. B. Kaner, and G. G. Wallace, "Processable aqueous dispersions of graphene nanosheets.," *Nat. Nanotechnol.*, vol. 3, no. 2, pp. 101–5, Feb. 2008.

[28] D. R. Dreyer, S. Park, C. W. Bielawski, and R. S. Ruoff, "The chemistry of graphene oxide.," *Chem. Soc. Rev.*, vol. 39, no. 1, pp. 228–240, 2010.

[29] B. P. COOK and E. G. STEWARD, "Graphitization in oriented carbons," *Zeitschrift für Krist. - Cryst. Mater.*, vol. 114, no. 1–6, Jan. 1960.

[30] A. Buchsteiner, A. Lerf, and J. Pieper, "Water Dynamics in Graphite Oxide Investigated with Neutron Scattering," *J. Phys. Chem. B*, vol. 110, no. 45, pp. 22328–22338, Nov. 2006.

[31] S. Stankovich, D. A. Dikin, R. D. Piner, K. A. Kohlhaas, A. Kleinhammes, Y. Jia, Y. Wu, S. T. Nguyen, and R. S. Ruoff, "Synthesis of graphene-based nanosheets via chemical reduction of exfoliated graphite oxide," *Carbon N. Y.*, vol. 45, no. 7, pp. 1558–1565, 2007.

[32] S. Stankovich, R. D. Piner, X. Chen, N. Wu, S. T. Nguyen, R. S. Ruoff, and Y. Talmon, "Stable aqueous dispersions of graphitic nanoplatelets via the reduction of exfoliated graphite oxide in the presence of poly(sodium 4-styrenesulfonate)," *J. Mater. Chem.*, vol. 16, no. 2, pp. 155–158, 2006.

[33] J. I. Paredes, S. Villar-Rodil, A. Martínez-Alonso, and J. M. D. Tascón, "Graphene Oxide Dispersions in Organic Solvents," *Langmuir*, vol. 24, no. 19, pp. 10560–10564, Oct. 2008.

[34] T. Ramanathan, A. A. Abdala, S. Stankovich, D. A. Dikin, M. Herrera-Alonso, R. D. Piner, D. H. Adamson, H. C. Schniepp, X. Chen, R. S. Ruoff, S. T. Nguyen, I. A. Aksay, R. K. Prud'Homme, and L. C. Brinson, "Functionalized graphene sheets for polymer nanocomposites," *Nat. Nanotechnol.*, vol. 3, no. 6, pp. 327–331, Jun. 2008.

[35] H. C. Schniepp, J.-L. Li, M. J. McAllister, H. Sai, M. Herrera-Alonso, D. H. Adamson, R. K. Prud'homme, R. Car, D. A. Saville, and I. A. Aksay, "Functionalized Single Graphene Sheets Derived from Splitting Graphite Oxide," *J. Phys. Chem. B*, vol. 110, no. 17, pp. 8535–8539, May 2006.

[36] H. Liu, H. Wang, and X. Zhang, "Facile fabrication of freestanding ultrathin reduced graphene oxide membranes for water purification," *Adv. Mater.*, vol. 27,

no. 2, pp. 249–254, 2015.

[37] Y. Si and E. T. Samulski, “Synthesis of water soluble graphene.,” *Nano Lett.*, vol. 8, no. 6, pp. 1679–82, Jun. 2008.

[38] S. Stankovich, D. A. Dikin, G. H. B. Dommett, K. M. Kohlhaas, E. J. Zimney, E. A. Stach, R. D. Piner, S. T. Nguyen, and R. S. Ruoff, “Graphene-based composite materials.,” *Nature*, vol. 442, no. 7100, pp. 282–6, Jul. 2006.

[39] G. Wang, J. Yang, J. Park, X. Gou, B. Wang, H. Liu, and J. Yao, “Facile Synthesis and Characterization of Graphene Nanosheets,” *J. Phys. Chem. C*, vol. 112, no. 22, pp. 8192–8195, Jun. 2008.

[40] W.-S. Hung, Q.-F. An, M. De Guzman, H.-Y. Lin, S.-H. Huang, W.-R. Liu, C.-C. Hu, K.-R. Lee, and J.-Y. Lai, “Pressure-assisted self-assembly technique for fabricating composite membranes consisting of highly ordered selective laminate layers of amphiphilic graphene oxide,” *Carbon N. Y.*, vol. 68, pp. 670–677, Mar. 2014.

[41] L. Yu, Y. Zhang, B. Zhang, J. Liu, H. Zhang, and C. Song, “Preparation and characterization of HPEI-GO/PES ultrafiltration membrane with antifouling and antibacterial properties,” *J. Memb. Sci.*, vol. 447, pp. 452–462, Nov. 2013.

[42] H. W. Kim, H. W. Yoon, S.-M. Yoon, B. M. Yoo, B. K. Ahn, Y. H. Cho, H. J. Shin, H. Yang, U. Paik, S. Kwon, J.-Y. Choi, and H. B. Park, “Selective Gas Transport Through Few-Layered Graphene and Graphene Oxide Membranes,” *Science (80-.).*, vol. 342, no. 6154, pp. 91–95, Oct. 2013.

[43] Y. Feng, C.-G. Hu, M.-L. Qi, R.-N. Fu, and L.-T. Qu, “Separation performance of graphene oxide as stationary phase for capillary gas chromatography,” *Chinese Chem. Lett.*, vol. 26, no. 1, pp. 47–49, 2015.

[44] Y. H. Yang, L. Bolling, M. a. Priolo, and J. C. Grunlan, “Super gas barrier and selectivity of graphene oxide-polymer multilayer thin films,” *Adv. Mater.*, vol. 25, no. 4, pp. 503–508, 2013.

[45] M. Bhadra, S. Roy, and S. Mitra, “Desalination across a graphene oxide membrane via direct contact membrane distillation,” *Desalination*, vol. 378, pp. 37–43, 2016.

[46] H. M. Hegab and L. Zou, “Graphene oxide-assisted membranes : Fabrication and potential applications in desalination and water puri fi cation,” vol. 484, pp. 95–106, 2015.

[47] J. Yin, G. Zhu, and B. Deng, “Graphene oxide (GO) enhanced polyamide (PA) thin-film nanocomposite (TFN) membrane for water purification,” *Desalination*, vol. 379, pp. 93–101, 2016.

[48] S. Li, X. Lu, Y. Xue, J. Lei, T. Zheng, and C. Wang, “Fabrication of polypyrrole/graphene oxide composite nanosheets and their applications for Cr(VI) removal in aqueous solution,” *PLoS One*, vol. 7, no. 8, 2012.

[49] P. Sun, M. Zhu, K. Wang, M. Zhong, J. Wei, D. Wu, Z. Xu, and H. Zhu, "Selective ion penetration of graphene oxide membranes.," *ACS Nano*, vol. 7, no. 1, pp. 428–37, Jan. 2013.

[50] M. Liu, C. Chen, J. Hu, X. Wu, and X. Wang, "Synthesis of magnetite/graphene oxide composite and application for cobalt(II) removal," *J. Phys. Chem. C*, vol. 115, no. 51, pp. 25234–25240, 2011.

[51] A. Nicolaï, B. G. Sumpter, and V. Meunier, "Tunable water desalination across graphene oxide framework membranes.," *Phys. Chem. Chem. Phys.*, vol. 16, no. 18, pp. 8646–54, May 2014.

[52] S. G. S. H. Kim, D. H. Hyeon, J. H. Chun, and B.-H. Chun, "Novel thin nanocomposite RO membranes for chlorine resistance," *Desalin. Water Treat.*, vol. 51, no. March 2015, pp. 6338–6345, 2013.

[53] C. Zhao, X. Xu, J. Chen, and F. Yang, "Effect of graphene oxide concentration on the morphologies and antifouling properties of PVDF ultrafiltration membranes," *J. Environ. Chem. Eng.*, vol. 1, no. 3, pp. 349–354, Sep. 2013.

[54] Y. Han, Z. Xu, and C. Gao, "Ultrathin Graphene Nanofi ltration Membrane for Water Purifi cation," pp. 3693–3700, 2013.

[55] R. K. Joshi, P. Carbone, F. C. Wang, V. G. Kravets, Y. Su, I. V Grigorieva, and H. A. Wu, "Precise and ultrafast molecular sieving through graphene oxide membranes," pp. 1–13.

[56] B. Mi, "Graphene Oxide Membranes for Ionic and Molecular Sieving," vol. 343, no. February, pp. 740–742, 2014.

[57] S. Park, D. A. Dikin, S. T. Nguyen, and R. S. Ruoff, "Graphene Oxide Sheets Chemically Cross-Linked by Polyallylamine," pp. 6–9, 2009.

[58] N. Hu, L. Meng, R. Gao, Y. Wang, J. Chai, Z. Yang, and E. S. Kong, "A Facile Route for the Large Scale Fabrication of Graphene Oxide Papers and Their Mechanical Enhancement by Cross-linking with Gluta- raldehyde," vol. 3, no. 4, pp. 215–222, 2011.

[59] T. H. Tight, "Unimpeded Permeation of Water," vol. 335, no. January, pp. 442–444, 2012.

[60] K. Sungjin Lee, G. Bozoklu, W. Cai, Ḱ. S. T. Nguyen, and R. S. Ruoff, "Graphene Oxide Papers Modified by Ions, Divalent Mechanical, Enhancing Cross-linking," *Prop. Chem. Park*, vol. 2, no. 3, 2014.

[61] T. Huang, L. Zhang, H. Chen, and C. Gao, "hybrid fi lm containing cipro fl oxacin : one-step preparation , controlled drug release and," *J. Mater. Chem. B Mater. Biol. Med.*, vol. 3, pp. 1605–1611, 2015.

[62] R. Manager, R. D. Export, and C. Only, "Graphene oxide – TiO 2 composite

filtration membranes and their potential application for water purification," 2016.

[63] S. Liu, T. H. Zeng, M. Hofmann, E. Burcombe, J. Wei, R. Jiang, J. Kong, and Y. Chen, "Antibacterial activity of graphite, graphite oxide, graphene oxide, and reduced graphene oxide: membrane and oxidative stress.," *ACS Nano*, vol. 5, no. 9, pp. 6971–80, Sep. 2011.

[64] Y. Gao, M. Hu, and B. Mi, "Membrane surface modification with TiO2–graphene oxide for enhanced photocatalytic performance," *J. Memb. Sci.*, vol. 455, pp. 349–356, Apr. 2014.

[65] F. Perreault, M. E. Tousley, and M. Elimelech, "Thin-Film Composite Polyamide Membranes Functionalized with Biocidal Graphene Oxide Nanosheets," *Environ. Sci. Technol. Lett.*, vol. 1, no. 1, pp. 71–76, Jan. 2014.

[66] C. Zhao, L. Xing, J. Xiang, L. Cui, J. Jiao, and H. Sai, "Particuology Formation of uniform reduced graphene oxide films on modified PET substrates using drop-casting method," *Particuology*, vol. 17, pp. 66–73, 2014.

[67] K. Goh, L. Setiawan, L. Wei, R. Si, A. G. Fane, R. Wang, and Y. Chen, "Graphene oxide as effective selective barriers on a hollow fi ber membrane for water treatment process," *J. Memb. Sci.*, vol. 474, pp. 244–253, 2015.

[68] S. Xia, L. Yao, Y. Zhao, N. Li, and Y. Zheng, "Preparation of graphene oxide modified polyamide thin film composite membranes with improved hydrophilicity for natural organic matter removal," *Chem. Eng. J.*, vol. 280, pp. 720–727, 2015.

[69] M. Hu and B. Mi, "Enabling graphene oxide nanosheets as water separation membranes," *Environ. Sci. Technol.*, vol. 47, no. 8, pp. 3715–3723, 2013.

[70] M. Hu and B. Mi, "Layer-by-layer assembly of graphene oxide membranes via electrostatic interaction," *J. Memb. Sci.*, vol. 469, pp. 80–87, 2014.

[71] M. Bhadra, S. Roy, and S. Mitra, "Desalination across a graphene oxide membrane via direct contact membrane distillation," *DES*, vol. 378, pp. 37–43, 2016.

[72] H. M. Hegab, Y. Wimalasiri, M. Ginic-markovic, and L. Zou, "Improving the fouling resistance of brackish water membranes via surface modi fi cation with graphene oxide functionalized chitosan," *DES*, vol. 365, pp. 99–107, 2015.

[73] Z. Wang, H. Yu, J. Xia, F. Zhang, F. Li, Y. Xia, and Y. Li, "Novel GO-blended PVDF ultrafiltration membranes," *Desalination*, vol. 299, pp. 50–54, 2012.

[74] J. Lee, H.-R. Chae, Y. J. Won, K. Lee, C.-H. Lee, H. H. Lee, I.-C. Kim, and J. Lee, "Graphene oxide nanoplatelets composite membrane with hydrophilic and antifouling properties for wastewater treatment," *J. Memb. Sci.*, vol. 448, pp. 223–230, Dec. 2013.

[75] Z. Xu, J. Zhang, M. Shan, Y. Li, B. Li, J. Niu, B. Zhou, and X. Qian, "Organosilane-functionalized graphene oxide for enhanced antifouling and

mechanical properties of polyvinylidene fluoride ultrafiltration membranes," *J. Memb. Sci.*, vol. 458, pp. 1–13, May 2014.

[76] H. Zhao, L. Wu, Z. Zhou, L. Zhang, and H. Chen, "Improving the antifouling property of polysulfone ultrafiltration membrane by incorporation of isocyanate-treated graphene oxide.," *Phys. Chem. Chem. Phys.*, vol. 15, no. 23, pp. 9084–92, Jun. 2013.

[77] B. M. Ganesh, A. M. Isloor, and a. F. Ismail, "Enhanced hydrophilicity and salt rejection study of graphene oxide-polysulfone mixed matrix membrane," *Desalination*, vol. 313, pp. 199–207, 2013.

[78] S. Zinadini, A. A. Zinatizadeh, M. Rahimi, V. Vatanpour, and H. Zangeneh, "Preparation of a novel antifouling mixed matrix PES membrane by embedding graphene oxide nanoplates," *J. Memb. Sci.*, vol. 453, pp. 292–301, 2014.

[79] M. Jun, S. Phuntsho, T. He, G. M. Nisola, L. D. Tijing, X. Li, G. Chen, W. Chung, and H. Kyong, "Graphene oxide incorporated polysulfone substrate for the fabrication of fl at-sheet thin- fi lm composite forward osmosis membranes," *J. Memb. Sci.*, vol. 493, pp. 496–507, 2015.

[80] X. Liu, J. Duan, J. Yang, T. Huang, N. Zhang, Y. Wang, and Z. Zhou, "Hydrophilicity , morphology and excellent adsorption ability of poly (vinylidene fluoride) membranes induced by graphene oxide and polyvinylpyrrolidone," *Colloids Surfaces A Physicochem. Eng. Asp.*, vol. 486, pp. 172–184, 2015.

[81] Q.-Z. Luo, N. D'Angelo, and R. L. Merlino, "Shock formation in a negative ion plasma," *Phys. Plasmas*, vol. 5, no. 8, pp. 2868–2870, 1998.

[82] E. M. Liston, L. Martinu, and M. R. Wertheimer, "Plasma surface modification of polymers for improved adhesion: a critical review," *J. Adhes. Sci. Technol.*, vol. 7, no. 10, pp. 1091–1127, Jan. 1993.

[83] A. C. Fozza, J. E. Klemberg-Sapieha, and M. R. Wertheimer, "Vacuum Ultraviolet Irradiation of Polymers," *Plasmas Polym.*, vol. 4, no. 2/3, pp. 183–206, 1999.

[84] C. Bichler, T. Kerbstadt, H.-C. Langowski, and U. Moosheimer, "Plasma-modified interfaces between polypropylene films and vacuum roll-to-roll coated thin barrier layers," *Surf. Coatings Technol.*, vol. 112, no. 1, pp. 373–378, 1999.

[85] T. R. Gengenbach and H. J. Griesser, "Post-deposition ageing reactions differ markedly between plasma polymers deposited from siloxane and silazane monomers," *Polymer (Guildf).*, vol. 40, no. 18, pp. 5079–5094, 1999.

[86] "Functionalization Methods for Membrane."

[87] S. Laboratories and R. April, "Plasma Modification of Poly(ether sulfone)," pp. 5498–5503, 1994.

[88] M. L. Steen, A. C. Jordan, and E. R. Fisher, "Hydrophilic modification of

polymeric membranes by low temperature H 2 O plasma treatment," vol. 204, pp. 341–357, 2002.

[89] J. Feng, G. Wen, W. Huang, and E. Kang, "Influence of oxygen plasma treatment on poly (ether sulphone) films," vol. 91, pp. 12–20, 2006.

[90] K. S. Kim, K. H. Lee, K. Cho, and C. E. Park, "Surface modification of polysulfone ultrafiltration membrane by oxygen plasma treatment," vol. 199, pp. 135–145, 2002.

[91] D. S. Wavhal and E. R. Fisher, "Modification of polysulfone ultrafiltration membranes by CO 2 plasma treatment," vol. 172, pp. 189–205, 2005.

[92] A. Kaynak, T. Mehmood, X. J. Dai, K. Magniez, and A. Kouzani, "Study of radio frequency plasma treatment of PVDF film using Ar, O2 and (Ar + O2) gases for improved polypyrrole adhesion," *Materials (Basel).*, vol. 6, no. 8, pp. 3482–3493, 2013.

[93] R.-J. Zhao, W.-S. Wang, F.-F. Zhu, T. Liu, Y.-H. Li, and Y.-L. Bian, "Surface modification of PVDF membrane by simultaneously using low temperature plasma and ammonium carbonate solution," *Desalin. Water Treat.*, vol. 56, no. 9, pp. 2276–2283, 2015.

[94] S. Pei, J. Zhao, J. Du, W. Ren, and H.-M. Cheng, "Direct reduction of graphene oxide films into highly conductive and flexible graphene films by hydrohalic acids," *Carbon N. Y.*, vol. 48, no. 15, pp. 4466–4474, 2010.

[95] C. Mandolfino, E. Lertora, and C. Gambaro, "Effect of Cold Plasma Treatment on Surface Roughness and Bonding Strength of Polymeric Substrates," *Key Eng. Mater.*, vol. 611–612, no. MAY, pp. 1484–1493, 2014.

[96] D. Hegemann, H. Brunner, and C. Oehr, "Plasma treatment of polymers for surface and adhesion improvement," *Nucl. Instruments Methods Phys. Res. Sect. B Beam Interact. with Mater. Atoms*, vol. 208, pp. 281–286, 2003.

[97] N. Slepickova Kasalkova, P. Slepicka, Z. Kolska, and V. Svorcik, "Wettability and Other Surface Properties of Modified Polymers," in *Wetting and Wettability*, InTech, 2015.

[98] R. M. F. and and R. D. Short*, "Plasma Treatment of Polymers: The Effects of Energy Transfer from an Argon Plasma on the Surface Chemistry of Polystyrene, and Polypropylene. A High-Energy Resolution X-ray Photoelectron Spectroscopy Study," 1998.

[99] C. S. Tang, B. Shi, C. Liu, W. Bin Suo, and L. Gao, "Experimental characterization of shrinkage and desiccation cracking in thin clay layer," *Appl. Clay Sci.*, vol. 52, no. 1–2, pp. 69–77, 2011.

[100] H. Nahlawi and J. K. Kodikara, "Laboratory experiments on desiccation cracking of thin soil layers," *Geotech. Geol. Eng.*, vol. 24, no. 6, pp. 1641–1664, 2006.

[101] C. Mühlhan, S. Weidner, J. Friedrich, and H. Nowack, “Improvement of bonding properties of polypropylene by low-pressure plasma treatment,” *Surf. Coatings Technol.*, vol. 116–119, pp. 783–787, Sep. 1999.

[102] C. K. Chua and M. Pumera, “Chemical reduction of graphene oxide: a synthetic chemistry viewpoint.,” *Chem. Soc. Rev.*, vol. 43, no. 1, pp. 291–312, 2014.

[103] T. Yumura and A. Yamasaki, “Roles of water molecules in trapping carbon dioxide molecules inside the interlayer space of graphene oxides,” *Phys. Chem. Chem. Phys.*, vol. 16, no. 20, p. 9656, 2014.

[104] O. Akhavan and E. Ghaderi, “Toxicity of graphene and graphene oxide nanowalls against bacteria,” *ACS Nano*, vol. 4, no. 10, pp. 5731–5736, 2010.

[105] S. Liu, T. H. Zeng, M. Hofmann, E. Burcombe, J. Wei, R. Jiang, J. Kong, and Y. Chen, “Antibacterial Activity of Graphite, Graphite Oxide, Graphene Oxide, and Reduced Graphene Oxide: Membrane and Oxidative Stress,” *ACS Nano*, vol. 5, no. 9, pp. 6971–6980, Sep. 2011.

[106] Y. Tu, M. Lv, P. Xiu, T. Huynh, M. Zhang, M. Castelli, Z. Liu, Q. Huang, C. Fan, H. Fang, and R. Zhou, “Destructive extraction of phospholipids from Escherichia coli membranes by graphene nanosheets,” *Nat. Nanotechnol.*, vol. 8, no. 8, pp. 594–601, Jul. 2013.

Vitae

Name	:Omer Alnoor Osman Alameen
Nationality	:Sudanese
Date of Birth	:6/16/1990
Marital Status	: single
Email	:omer.alnoor90@hotmail.com
Telephone	: +24992326234 / +966533591509
Address	:Khartoum-Sudan
Academic Background	:Mechanical Engineer

Education

H.S.S.C 1997 from Nadir Ata private Secondary School, Khartoum.

B.sc 2012 in Mechanical Engineering from Khartoum University.

Joined King Fahd University of petroleum and Minerals in 2012 as M.sc student.

Completed M.sc (mechanical engineering) in 2017.